



UNIVERSIDAD DE INVESTIGACIÓN DE TECNOLOGÍA EXPERIMENTAL YACHAY

Escuela de Ciencias Biológicas e Ingeniería

**TÍTULO: Chemical characterization of six Thiadiazine
compounds with antimalarial activity and their cross-reactivity
in the humoral response**

Trabajo de integración curricular presentado como requisito para la
obtención del título de Bióloga

Autor:

Mishell Poleth Ortiz Jacome

Tutor:

Ph.D.- Lilian Maritza Spencer Valero

Co-Tutor:

Ph.D.-Hortensia Maria Rodríguez Cabrera

Urcuquí, Julio de 2021

SECRETARÍA GENERAL
(Vicerrectorado Académico/Cancillería)
ESCUELA DE CIENCIAS BIOLÓGICAS E INGENIERÍA
CARRERA DE BIOLOGÍA
ACTA DE DEFENSA No. UITEY-BIO-2021-00015-AD

A los 28 días del mes de junio de 2021, a las 11:30 horas, de manera virtual mediante videoconferencia, y ante el Tribunal Calificador, integrado por los docentes:

Presidente Tribunal de Defensa Dr. SANTIAGO VISPO, NELSON FRANCISCO , Ph.D.
Miembro No Tutor Dr. TELLKAMP TIETZ, MARKUS PATRICIO , Ph.D.
Tutor Dra. SPENCER VALERO, LILIAN MARITZA , Ph.D.

El(la) señor(ita) estudiante **ORTIZ JACOME, MISHHELL POLETH**, con cédula de identidad No. **1003173695**, de la **ESCUELA DE CIENCIAS BIOLÓGICAS E INGENIERÍA**, de la Carrera de **BIOLOGÍA**, aprobada por el Consejo de Educación Superior (CES), mediante Resolución **RPC-SO-37-No.438-2014**, realiza a través de videoconferencia, la sustentación de su trabajo de titulación denominado: **Chemical characterization of 6 thiadiazine compounds with antimalarial activity and their cross reactivity in the humoral response** , previa a la obtención del título de **BIÓLOGO/A**.

El citado trabajo de titulación, fue debidamente aprobado por el(los) docente(s):

Tutor Dra. SPENCER VALERO, LILIAN MARITZA , Ph.D.

Y recibió las observaciones de los otros miembros del Tribunal Calificador, las mismas que han sido incorporadas por el(la) estudiante.

Previamente cumplidos los requisitos legales y reglamentarios, el trabajo de titulación fue sustentado por el(la) estudiante y examinado por los miembros del Tribunal Calificador. Escuchada la sustentación del trabajo de titulación a través de videoconferencia, que integró la exposición de el(la) estudiante sobre el contenido de la misma y las preguntas formuladas por los miembros del Tribunal, se califica la sustentación del trabajo de titulación con las siguientes calificaciones:

Tipo	Docente	Calificación
Tutor	Dra. SPENCER VALERO, LILIAN MARITZA , Ph.D.	10,0
Miembro Tribunal De Defensa	Dr. TELLKAMP TIETZ, MARKUS PATRICIO , Ph.D.	9,7
Presidente Tribunal De Defensa	Dr. SANTIAGO VISPO, NELSON FRANCISCO , Ph.D.	10,0

Lo que da un promedio de: **9.9 (Nueve punto Nueve)**, sobre 10 (diez), equivalente a: **APROBADO**

Para constancia de lo actuado, firman los miembros del Tribunal Calificador, el/la estudiante y el/la secretario ad-hoc.

Certifico que en cumplimiento del Decreto Ejecutivo 1017 de 16 de marzo de 2020, la defensa de trabajo de titulación (o examen de grado modalidad teórico práctica) se realizó vía virtual, por lo que las firmas de los miembros del Tribunal de Defensa de Grado, constan en forma digital.



ORTIZ JACOME, MISHHELL POLETH
Estudiante

NELSON
FRANCISCO
SANTIAGO
VISPO

Firmado digitalmente por
NELSON FRANCISCO
SANTIAGO VISPO
Fecha: 2021.06.28
13:14:50 -05'00'

Dr. SANTIAGO VISPO, NELSON FRANCISCO , Ph.D.
Presidente Tribunal de Defensa

LILIAN
MARITZA
SPENCER
VALERO

Firmado digitalmente
por LILIAN MARITZA
SPENCER VALERO
Fecha: 2021.06.28
21:12:29 -05'00'

Dra. SPENCER VALERO, LILIAN MARITZA , Ph.D.
Tutor



Firmado electrónicamente por:
**MARKUS PATRICIO
TELLKAMP TIETZ**

Dr. TELLKAMP TIETZ, MARKUS PATRICIO , Ph.D.

Miembro No Tutor

KARLA
ESTEFANIA
ALARCONFELIX

Firmado digitalmente
por KARLA ESTEFANIA
ALARCON FELIX

Fecha: 2021.06.28
12:45:33 -05'00'

ALARCON FELIX, KARLA ESTEFANIA
Secretario Ad-hoc



AUTORÍA

Yo, Mishell Poleth Ortiz Jacome, con cédula de identidad 1003173695, declaro que las ideas, juicios, valoraciones, interpretaciones, consultas bibliográficas, definiciones y conceptualizaciones expuestas en el presente trabajo; así como los procedimientos y herramientas utilizados en la investigación, son de absoluta responsabilidad de la autora del trabajo de integración curricular. Así mismo, me acojo a los reglamentos internos de la Universidad de Investigación de Tecnología Experimental Yachay.

Urcuquí, marzo de 2021.



Mishell Poleth Ortiz Jacome
CI: 1003173695

AUTORIZACIÓN DE PUBLICACIÓN

Yo, Mishell Poleth Ortiz Jacome, con cédula de identidad 1003173695, cedo a la Universidad de Investigación de Tecnología Experimental Yachay, los derechos de publicación de la presente obra, sin que deba haber un reconocimiento económico por este concepto. Declaro además que el texto del presente trabajo de titulación no podrá ser cedido a ninguna empresa editorial para su publicación u otros fines, sin contar previamente con la autorización escrita de la Universidad.

Asimismo, autorizo a la Universidad que realice la digitalización y publicación de este trabajo de integración curricular en el repositorio virtual, de conformidad a lo dispuesto en el Art. 144 de la Ley Orgánica de Educación Superior

Urququí, marzo de 2021.



Mishell Poleth Ortiz Jacome
CI: 1003173695

DEDICATION

To my parents, Armando Ortiz and Silvana Jacome, to my sister and brother, Clara and Bradley, and finally to my grandparents, Gerardo and Emma for supporting me unconditionally.

Mishell Poleth Ortiz Jacome

ACKNOWLEDGMENTS

First of all, I want to thank my tutor, Lilian Spencer, for giving me all the support and patience during the development of the thesis. Also, I want to thank my co-tutor Hortensia Rodriguez, for guiding and motivating me.

To Dr. Beatriz Pernía Santos from the University of Guayaquil for helping us with the statistical analysis of the cross-reactivity results.

To Karen Sanchez from University of Yachay Tech for helping us in ELISA experiments.

To my parents, Armando and Silvana, and my sister Clara, and my brother Bradley who have given me all their love, support and company.

Finally, I thank my friends: Kimberly, Vinicio, Andrea, Catalina, Fernando, Dalena, Katy, Yoshi, and Brian for supporting me and encouraging me in the most difficult moments.

Mishell Poleth Ortiz Jacome

RESUMEN

La malaria es una infección parasitaria causada por un protozoo del género Plasmodium, transmitido a los humanos por mosquitos hembra del género Anopheles que pican. Según la Organización Mundial de la Salud (OMS), los casos de malaria en todo el mundo disminuyeron de 238 millones de casos en 2000 a 230 millones de casos en 2019. Además, en 2000 en todo el mundo se notificaron 736 000 muertes, en comparación con 409 000 muertes estimadas en 2019, lo que significa que la malaria sigue constituyendo un problema de salud mundial. La cloroquina es un fármaco muy utilizado en el tratamiento de la malaria. Durante más de 60 años, este fármaco se ha utilizado como antipalúdico en zonas endémicas y el uso excesivo ha provocado la resistencia del parásito a los fármacos. Por tanto, el parásito ha desarrollado farmacoresistencia frente a la cloroquina y sus derivados. En consecuencia, es crucial buscar nuevos medicamentos contra la malaria como tratamientos.

En estudios anteriores, seis derivados de tetrahidro- (2H) -1,3,5-tiadiazina-2-tiona (THTT) se evaluaron in vivo con dos cepas de malaria en roedores y algunas de ellas mostraron varias actividades antipalúdicas. El objetivo de este trabajo fue caracterizar químicamente seis derivados de tetrahidro- (2H) -1,3,5-tiadiazina-2-tiona (bis-THTT) por punto de fusión (pf), IR (espectroscopía infrarroja), UHPLC (ultra -cromatográfica líquida de alto rendimiento) y UV / Vis (Ultravioleta / Visible) y su evaluación de la respuesta humoral con sueros hiperinmunes mediante prueba ELISA indirecta (Ensayo inmunoabsorbente ligado a enzimas). Los sueros hiperinmunes también se utilizaron para evaluar la reactividad cruzada entre los compuestos como antígenos mediante la prueba ELISA indirecta.

Además, se realizó una prueba de antígenos combinados en la prueba ELISA indirecta entre los dos antígenos previamente reconocidos por los sueros hiperinmunes y la prueba ELISA indirecta para evaluar las estructuras químicas policlonales de los anticuerpos de los sueros de forma indirecta.

Los resultados de la evaluación humoral mediante el uso de ELISA indirecto muestran que los compuestos JH1, JH3 y JH4 reaccionan con casi todos ellos. Además, los antígenos de los compuestos JH4, JH5 y JH6 estimulan el sistema inmunológico de los ratones BALB / C y presentan la mayor absorbancia (0.080, 0.066 y 0.118 O.D., respectivamente). Por otro lado, los antígenos con menor estimulación de respuesta humoral son la cloroquina y JH1 (0,027, 0,044 D.O., respectivamente).

Finalmente, sugerimos que las mejores combinaciones de dos antígenos como terapia combinada serían: JH1 + JH3, JH1 + JH4, JH2 + JH3 y JH2 + JH4 porque comparten absorbancias similares entre la mezcla de antígenos, mostrando un reconocimiento similar por los anticuerpos. y por compuestos.

Palabras clave: Paludismo, cloroquina, compuestos como tiadiazina, ELISA indirecto y caracterización química.

1. ABSTRACT

Malaria is a parasitic infection caused by a protozoan of the genus *Plasmodium*, transmitted to humans by female biting mosquitoes of the genus *Anopheles*. According to the World Health Organization (WHO), Malaria cases worldwide decreased from 238 million cases in 2000 to 230 million cases in 2019. Besides, in 2000 worldwide an estimated 736 000 deaths were reported, compared with 409 000 estimated deaths in 2019, which means Malaria still constitutes a global health problem. Chloroquine is a drug widely used in malaria treatment. For more than 60 years, this drug has been used as anti-malaria in endemic areas, and overuse has caused the parasite's drug resistance. Therefore, the parasite has developed drug resistance against the chloroquine and its derivatives. In consequence, it is crucial to search for new anti-malaria drugs as treatments.

In previous studies, six derivatives of tetrahydro- (2H)-1,3,5-thiadiazine-2-thione (THTT) were evaluated *in vivo* with two strains of rodent malaria and some of them showed several anti-malaria activities. The aim of this work was to chemically characterize six derivatives of tetrahydro- (2H)-1,3,5-thiadiazine-2-thione (bis-THTT) by melting point (mp), IR (Infrared spectroscopy), UHPLC (ultra-high-performance liquid chromatographic), and UV/Vis (Ultraviolet/Visible) technique and their evaluation of humoral response with hyper-immune sera by indirect ELISA test (Enzyme-Linked-Immunosorbent Assay). The hyper-immune sera were also used to evaluate cross-reactivity between the compounds as antigens by indirect ELISA test.

Furthermore, a combined antigens test was performed in the indirect ELISA test between the two antigens previously recognized by the hyper-immune sera and the indirect ELISA test to evaluate the polyclonal's chemical structures antibodies from sera indirectly.

The humoral evaluation results through the use of indirect ELISA shows that compounds JH1, JH3, and JH4 react with almost all of them. Besides, the compounds JH4, JH5, and JH6 antigens stimulate the BALB/ C mice's immune system and present the highest absorbance (0.080, 0.066, and 0.118 O.D., respectively). On the other hand, the antigens with less humoral response stimulation are chloroquine and JH1 (0.027, 0.044 O.D., respectively).

Finally, we suggest that the best combinations of two antigens as a combined therapy would be: JH1 + JH3, JH1 + JH4, JH2 + JH3, and JH2 + JH4 because they share similar absorbances between the mixture of antigens, showing similar recognition by antibodies and by compounds.

Key words: Malaria, Chloroquine, compounds like Thiadiazine, Indirect ELISA and chemical characterization.

GENERAL INDEX

1. ABSTRACT	9
INTRODUCTION	18
2.1 The life cycle of Malaria	19
2.2 Heterocyclic compound	20
2.3 Antimalarial drugs	21
2.4 Antimalarial drugs combinate or single	22
2.5 Derivatives of Chloroquine and Artemisinin	23
2.6 Mode of action of Chloroquine and Artemisinin	24
2.7 Antimalarial resistance	25
2.8 Humoral response in malaria	26
2.9 Cross-reactivity assay in the malaria evaluation	27
3.0 Tetrahydro-2h-1,3,5-thiadiazine-2-thione (THTT) derivatives	28
3.1 Chemical structure of bis-tetrahydro-2H-1,3,5-thiadiazine-2-thione (THTT) and its origin	29
2. PROBLEM STATEMENT	29
3. HYPOTHESIS	30
4. OBJECTIVES	30
4.1 General Objective	30
4.2 Specific Objectives	30
5. MATERIALS AND METHODS	30
5.1 Compounds derived from bis-THTT	30

5.2	Melting point	33
5.3	Fourier-transform infrared spectroscopy	33
5.4	UHPLC and UV/Vis	33
5.5	Indirect ELISA test using the experimental compounds as antigens	33
5.6	Indirect ELISA test with two combination of antigens	34
5.7	Statistical analysis	35
6.	RESULTS AND DISCUSSION	35
6.1	Characterization of compounds derived by bis-THTT	35
6.1.1	Melting point	35
6.1.2	FT-IR of bis-tetrahydro-2(1H)-thiadiazine-2-thiones (JH1-JH6)in experimental compound	36
6.1.3	UV/Vis spectroscopy of bis-tetrahydro-2(1H)-thiadiazine-2-thiones (JH1-JH6)	37
6.1.4	UHPLC of bis-tetrahydro-2(1H)-thiadiazine-2-thiones (JH1-JH6)	39
6.2	Evaluation of the experimental compounds by indirect ELISA test	42
6.2.1	Solubility behavior of THTTs in DMSO.	42
6.2.2	Determination of time reaction of each experimental compound in ELISA test.	43
6.2.3	Cross-reactivity between experimental compounds	47
6.2.4	Determination of time reaction of each combination of experimental compounds in ELISA test.	51
6.2.5	Evaluation of cross-reactivity between the combination of two compounds as antigens in indirect ELISA	52
7.	CONCLUSION	55
8.	REFERENCES	56
9.	ANNEXES	61
	Annex 1	61
	Annex 2	61
	Annex 3	62
	Annex 5	63
	Annex 6	63

Annex 7	64
Annex 8	64
Annex 9	65
Annex 10	65
Annex 11	66
Annex 12	66
Annex 13	67
Annex 14	67
Annex 15	68
Annex 16	68
Annex 17	69
Annex 18	69

INDEX OF TABLES

Table 1. Drugs used for each species of <i>Plasmodium</i>	22
Table 2. Dome antimalarial drugs with their respective resistance polymorphisms	26
Table 3. Distribution of antigens and sera in the ELISA plate 1	34
Table 4. Distribution of combination of antigens in the ELISA plate 1	34
Table 5. Melting point of compounds (JH1, JH2, JH3, JH4, JH5, JH6)	35
Table 6. Distribution of compounds diluted with DMSO	43
Table 7. Cross-reactivity of antibody with antigen, where + means the presence of cross-reactivity and – means there is not cross reactivity.	50
Table 8. Cross-reactivity of antibody with antigen from highest to the lowest humoral response.	51

INDEX OF FIGURES

Figure 1. The life cycle of <i>Plasmodium</i> in humans.....	20
Figure 2. Heterocyclic motifs used antimalarial agents.	22
Figure 3. Chloroquine structure.....	24
Figure 4. Artemisinin structure.....	24
Figure 5. The cellular immune response of chloroquine action.	25
Figure 6. Chemical structure of compounds derived from alkyl-linked bis-(2-thioxo-[1,3,5]thiadiazinan-3-yl) carboxylic acids.....	29
Figure 7. Procedure for obtaining bis-THTT.....	29
Figure 8. Chemical structure of JH1 compound.....	31
Figure 9. Chemical structure of JH2 compound.....	31
Figure 10. Chemical structure of JH3 compound.....	31
Figure 11. Chemical structure of JH4 compound.....	32
Figure 12. Chemical structure of JH5 compound.....	32
Figure 13. Chemical structure of JH6 compound.....	32
Figure 14. FT-IR absorption spectra of JH1 compound.....	33
Figure 15. FT-IR absorption spectra of JH2 compound.....	37
Figure 16. UV/Vis absorption spectra of JH1 compound	38
Figure 17. UV/Vis absorption spectra of JH2 compound.	38
Figure 18. UHPLC profile of JH1 compound	39
Figure 19. UHPLC profile of JH2 Compound	40

Figure 20. UHPLC profile of JH3 compound	40
Figure 21. UHPLC profile of JH4 compound	41
Figure 22. UHPLC profile of JH5 compound	41
Figure 23. UHPLC profile of JH6 compound	42
Figure 24. Indirect ELISA results, antibody (pre-immune called PIS and hyper-immune sera cqs) reactivity with antigen (CQ compound)..	44
Figure 25. Indirect ELISA results, antibody (pre-immune called PIS and hyper-immune sera JH1S) reactivity with antigen (JH1 compound)..	44
figure 26. Indirect ELISA results, antibody (pre-immune called PIS and hyper-immune sera JH2S) reactivity with antigen (JH2 compound)	45
Figure 27. Indirect ELISA results, antibody (pre-immune called PIS and hyper-immune sera JH3S) reactivity with antigen (JH3 compound)..	45
Figure 28. Indirect ELISA results, antibody (pre-immune called PIS and hyper-immune sera JH4S) reactivity with antigen (JH4 compound).....	46
Figure 29. Indirect ELISA results, antibody (pre-immune called PIS and hyper-immune sera JH5S) reactivity with antigen (JH5 compound).....	46
Figure 30. Indirect ELISA results, antibody (pre-immune called PIS and hyper-immune sera JH6S) reactivity with antigen (JH6 compound).....	47
Figure 31. Results of indirect ELISA with 10 µg/ml concentration of antigens (CQ, JH1, JH2, JH3, JH4 and JH6 compounds).....	49
Figure 32. Indirect ELISA results, antibody (pre-immune called pis and hyper-immune JH1, JH3) reactivity with antigen (JH1+JH3 compounds).....	52
Figure 33. Results of indirect ELISA at 20 minutes, with 10 µg/ml concentration of combination of antigens (CQ+JH1, CQ+JH4, JH1+JH3, JH1+JH4, JH2+JH3, JH2+JH4, JH4+JH3, JH5+JH4, JH5+JH6, JH6+JH4, JH6+JH3)	53

INDEX OF ABBREVIATIONS

ABTS: 2,2'-azino-bis (3-ethylbenzthiazoline-6-sulfuric acid)
ACN: Acetonitrile
ACT: Artemisinin combination therapy
AMA: Apical Membrane Antigen
APC: Antigen presentation cell
ATR: Total Reflection Attenuated
Bis-THTT: Bis-tetrahydro-(2H)-1,3,5-thiadiazine-2-thione.
BSA: Bovine serum albumin
CQ: Chloroquine
DMF: Dimethylformamide
DMSO: Dimethyl-sulfoxide
DNA: Deoxyribonucleic acid
ELISA: Enzyme-linked immunosorbent assay
GLURP: Glutamate rich Plasmodium falciparum
Gly: Glycine
IgA: Immunoglobulins A
IgG: Immunoglobulins G
IgM: Immunoglobulins M
IR: Infrared spectroscopy
Leu: Leucine
mAb: Monoclonal antibody
Min: Minutes
Mp: Melting point
MSP: Merozoite Surface Protein
P: Plasmodium
PBS/T: Phosphate buffered saline and Tween 20
PBS: Phosphate buffered saline
PfCRT: Plasmodium falciparum chloroquine resistance)
Pfk13: Phosphatidylinositol-3-kinase
PPQ: Piperaquine
RBCs: Red Blood Cells
RNA: Ribonucleic acid
SAR: Structure-activity relationship
T: Trypanosoma
TLR: Toll-like receptor (TLR)
UHPLC: Ultra-high-performance liquid chromatographic
UV/Vis: Ultraviolet/Visible
Val: Valine
WHO: World Health Organization

INTRODUCTION

Malaria is transmitted by the bite of female *Anopheles* mosquitos when they suck up the blood and introduces the *Plasmodium* parasite. The parasite is a protozoan of the phylum Apicomplexa (Phillips et al., 2017). According to a report in 2018 of the World Health Organization (WHO), 67% of malaria deaths were reported in the most vulnerable members of society, children aged under five years. Other vulnerable hosts are pregnant women whose exposure to this parasite causes prematurity, low birth-weight, and even infant mortality (World Health Organization, 2019). The incidence rate of malaria cases worldwide was 238 million cases in 2000, and 230 million cases in 2019. Besides, in 2000 an estimated 736 000 deaths were reported from malaria were worldwide, compared with 409 000 estimated deaths in 2019 (World Health Organization, 2020).

In 2018 the WHO reported that 67% of malaria deaths were occurred in the most vulnerable human host: the children aged under five. Other vulnerable hosts are pregnant women because their exposure to this parasite causes prematurity, low birth weight, and infant mortality (World Health Organization, 2019). The symptoms that develop malaria in the human body are violent fever for six to eight hours, fever every 3 to 4 days, paroxysms, muscle aches, and digestive symptoms. In severe cases of malaria, which is due to microvascular obstruction, severe anemia and various manifestations of multi-organ damage, even cerebral malaria might occur (Phillips et al., 2017).

The genus *Plasmodium* consists of five species that infect humans: *Plasmodium vivax*, *P. ovale*, *P. malarie*, *P. falciparum*, and *Plasmodium knowlesi*. The most dangerous species that causes serious health problems are *P. falciparum* and *P. vivax*. In 2018, the highest prevalence reported of *P.falciparum* was in the African Region with 99.7%, followed by the Eastern Mediterranean Region with 71%, the Western Pacific Region with 65%, and Asian Region with 50%, in the population. On the other hand, most cases reported for *P.vivax* were in South-Eastern Asia with 53% and America up to 75% in the population (World Health Organization, 2019).

One of the problems in the last years has been antimalarial resistance. Consequently, the current drug efficiency decreases, so it is essential to study viable candidates to treat this disease that lead to finding new drugs. The development of new technologies is necessary for drug discovery research. The application of characterization techniques are melting point, IR (Infrared spectroscopy), UHPLC (ultra-high-performance liquid chromatography), and UV/Vis (ultraviolet/visible) allow to confirm the structure of lead molecule bioactive fractions and also contribute to determine the structure-activity relationship.

Different techniques are carried out for the chemical characterization, mentioned below those used in this work.

Melting point (mp) is a physical property that helps identifying a compound and can establish the sample's relative purity (Nichols, 2020). FT-IR spectroscopy is used for the characterization and identification of functional groups present in an unknown mixture. Also, this method contains a library of known compounds that can be compared with the spectrum of a novel analyzed compound (Koparde et al., 2019).

Chromatography techniques are separation procedures based on the difference in polarity, size, or charge of molecules. During chromatography, the analyte in the solvent moves through the stationary phase that acts as a sieving material. Then, the molecule proceeds further through a molecular sieve that, as a result, gets separated. HPLC is a technique used for isolation, identification. This technique determine purity and should result in a clean, sharp peak of a known sample at a specific retention times. UHPLC is similar to

HPLC, but higher pressures are applied. Their efficacy, resolution, and efficiency are involved with the diminution of the particle size to fill the column. Also, the analysis speed and maximum capacity are better than HPLC (Rios, 2019).

The Ultra-High-Performance Liquid Chromatography (UHPLC) is a technique to separate the components of a mixture and establish the purity of the compounds. HPLC generally uses UV detectors because they have high sensitivity (Koparde et al., 2019). The UV/Vis spectroscopy principle is based on the absorption of ultraviolet and visible light by chemical compounds, which results in the spectrum. UV/Vis spectroscopy is currently only marginally relevant to structure elucidation but would be usefully applied to UV/Vis detectors like those used in HPLC and UHPLC chromatographic techniques.

Another aspect of relevance is the immunological evaluation of the candidate drug to determine their effect on the biological system, as in the experimental mouse model. Thus, the use of polyclonal antibodies in recognition of the compounds' chemical structure will allow us to determine the possible combined drug therapy to improve the treatment against the disease.

The concentration of biological compounds such as proteins is measured by techniques that use enzymes. One of the most commonly used one is the ELISA or enzyme immunoassay, which is frequently applied to diagnose diseases. Indirect ELISA is a test based on measuring the antigen, not by the primary antibody (polyclonal). This test is measured by the secondary antibody bound or conjugated to an enzyme, and the enzyme is unit its substrate. The substrate reacts with the enzyme and gives a color through a colorimetric chain reaction measured on a spectrophotometer, resulting in absorbance at a determinate wavelength (Aydin, 2015).

2.1 The life cycle of Malaria

Malaria is caused by a protozoan parasite of the phylum Apicomplexa, belonging to the genus *Plasmodium*. Five malaria species affect humans: *P. falciparum*, *P. vivax*, *P. ovale*, *P. malariae*, and the zoonotic *P. knowlesi*. Malaria develops within two hosts, an invertebrate (mosquito) and a vertebrate (human or monkey). The Malaria cycle presents four stages during their life cycle, which follow the following sequence: fertilization (sexual phase), sporogony (first asexual phase), hepatic schizogony (second asexual phase), and erythrocytic schizogony (third asexual phase) (Figure 1) (Knell, 1991).

This cycle starts when an infected female *Anopheles* mosquito sucks up blood from humans injecting sporozoites into the blood through their epidermal capillaries. The hepatic schizogony phase starts when sporozoites move through the bloodstream and invade the liver cells to develop into hepatic trophozoites. The trophozoites invade the hepatocytes and, through asexual multiplication, produce other stages called merozoites, which invade erythrocytes (Spencer et al., 2016). The erythrocytic schizogony phase occurs in the blood, where the merozoites multiply in red blood cells to become erythrocytic trophozoites. The erythrocytic trophozoites multiply and release 32 new merozoites in approximately 48 hours from a mature schizont, rupturing the cells; then, the erythrocytic cycle can be repeated with re-invasion of RBCs (Spencer et al., 2016).

The process of infection progresses when the Red Blood Cells (RBCs) burst and release merozoites, and some of them can develop into male (microgamete) or female (macrogamete) gametocytes. The cycle continues when a mosquito bites an infected human, ingesting some gametocytes to initiate the parasite's sexual stage in the mosquito's stomach. The male gamete combines with the female gamete to produce fertilization, producing a

diploid zygote (Knell, 1991). The zygote matures and transforms into a mobile ookinete, which stays in the stomach wall and becomes an oocyst. Finally, the oocyst grows and divides to produce thousands of invasive sporozoites, repeating the life cycle (Beck, 2006).

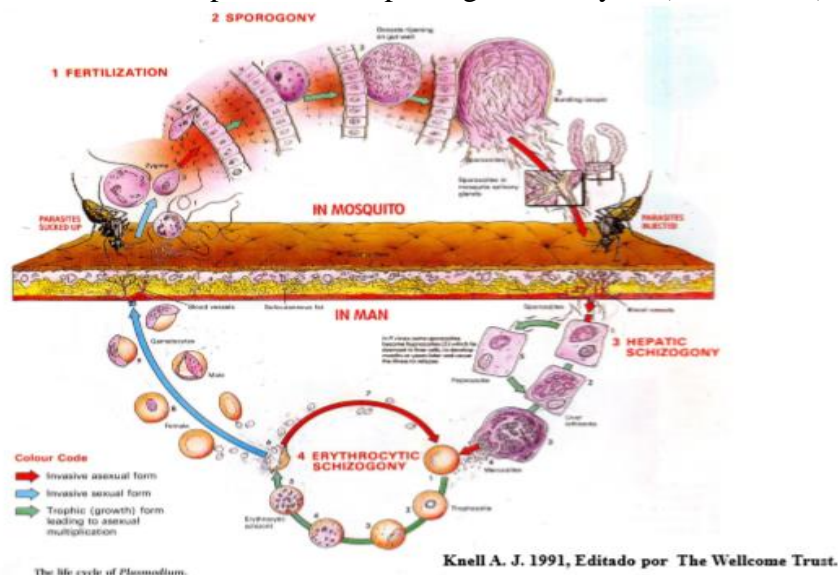


Figure 1. The life cycle of *Plasmodium* in humans (From Knell, 1991).

2.2 Heterocyclic compound

According to IUPAC, heterocyclic compounds are defined as “cyclic compounds having as ring member’s atoms of at least two different elements” (IUPAC, 2014). Their structure consists of one or more heterocycles, either isolated or fused, containing carbons, hydrogens, and heteroatoms like N, O, S, Se, and others (Barmade & Ghuge, 2018). The heterocyclic compounds’ physicochemical properties can be affected by the type and size of ring structures and the core scaffold's substituent groups (Martins et al., 2015). Heterocycles can be classified as aromatic and non-aromatic, where aromatic are found in many biologically active motifs and clinical drugs.

The heterocycles have been used for the development of many drugs for different health conditions. These compounds have many applications in medicinal chemistry and biology and occur naturally and non-naturally (Aljamali & Alfatlawi, 2015). Heterocycles are present in a broad range of organic compounds with natural origins, such as chlorophyll, hemoglobin, amino acids, DNA and RNA bases, vitamins, hormones, or may be synthetic, such as antibiotics, several dyes, and, alkaloids drugs (morphine, quinine, colchicine, codeine, and cocaine), among others (Aljamali & Alfatlawi, 2015; Barmade & Ghuge, 2018). Heterocyclic compounds have shown anti-bacterial, anti-viral, anti-fungal, anti-inflammatory, and anti-tumor activities. Non-aromatic compounds are of limited potential for the discovery of new drugs (Barmade & Ghuge, 2018). Heterocyclic compounds have a capacity of readily donating electrons and robust coordination abilities (Sabir et al., 2016). The experimental compounds bis-tetrahydro-(2H)-1,3,5-thiadiazine-2-thione derivatives used in the present research belong to the heterocyclic compounds. They are six-member heterocycles with nitrogen atoms in three and five positions, sulfur in one position 1, and a thione group in two.

2.3 Antimalarial drugs

Antimalarial drugs are chemical substances designed to prevent or treat malaria. Most antimalarial drugs target the erythrocytic stage of the malaria infection. Subsequently, the most used antimalarial drugs will be mentioned, from quinine to artemisinin therapy.

Quinine ($C_{20}H_{24}N_2O_2$), the first antimalarial drug, is derived from the bark of the *Cinchona ledgeriana* tree. The discovery of *Cinchona* bark in the 17th century was made in South America by Inca herbalists trying to treat fevers. This compound's composition was reported by Pelletier and Caventou in 1820, who isolated the alkaloids, cinchonine, and quinine. They subsequently discovered the correct dosage to administer to people causing their demand to overgrow to treat malaria (Knell, 1991). The action of quinine in the malaria parasite consists of being an intra-erythrocytic schizonticide, through the association with the heme polymer in the acidic food vacuole of *Plasmodium*, thus preventing polymerization by heme polymerase enzyme. This action producing an increase of the solubility of malarial pigment into the cell by an accumulation of toxic heme, which causes lysis of the parasite (National Center for Biotechnology Information, 2021).

For the past 50 years, the only antimalarial drugs were Mefloquine and other quinolone drugs (Noronha et al., 2020). In the mid-20th century, new synthetic chemicals to fight against Malaria appeared. The next-generation medicines that interfere with hemozoin (malarial pigment) formation are the combination of 4-aminoquinolines and amino-alcohols (Phillips et al., 2017). The most frequent drugs used for malaria are chloroquine and artemisinin therapies. Chloroquine (CQ) was discovered in Germany in 1930, belong to type 4-aminoquinoline, has been the safest drug used for many years (Knell, 1991). Chloroquine is now the most commonly used drug to treat malaria, especially for infections by *P. vivax*. This drug is used due to excellent clinical efficacy, limited host toxicity, ease of use and cost-effective synthesis (Phillips et al., 2017; Noronha et al., 2020) This drug does not allow the hemozoin, a product released during hemoglobin's proteolysis, to detoxify in the parasite digestive vacuole, thus producing a toxic effect and leading to death of the parasite (Noronha et al., 2020).

Artemisinin combined therapies (ACTs) are used to treat *Plasmodium falciparum*. This therapy combines an artemisinin derivative and quinine derivative (Phillips et al., 2017). Artemisinin is a tetracyclic 1,2,4-trioxane that contains an endoperoxide bridge, and sesquiterpene lactone produced by *Artemisia annua*, a wormwood herb (Noronha et al., 2020; Pinheiro et al., 2018). WHO suggests the application of five combined treatments based on artemisinin (Phillips et al., 2017). The following figure names various heterocyclic motifs to treat *Plasmodium* that demonstrate effectiveness as antimalarial agents: aminoquinolones, fused pyran scaffolds, quinazoline, and quinoxaline, indole, pyrimidine, pyrazoline, triazole, imidazole, isoxazole, isoquinoline, triazine, and pyrazole (Kalaria et al., 2018).

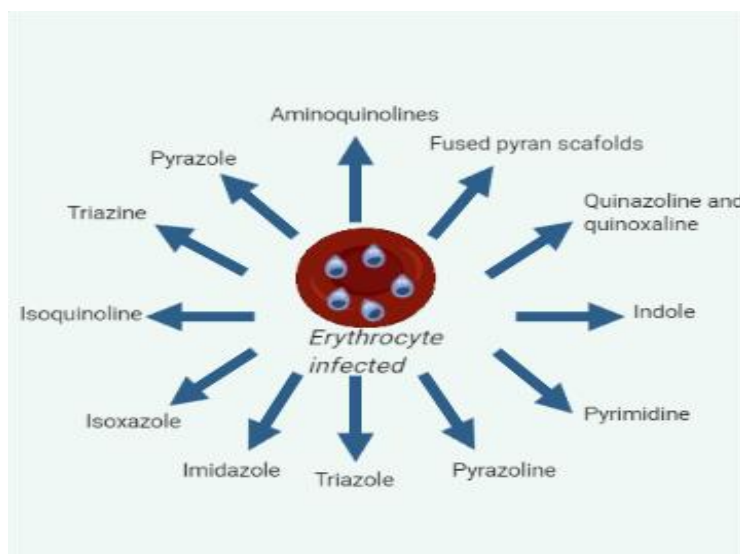


Figure 2. Heterocyclic motifs used antimalarial agents (Figure made by Mishell Ortiz).

2.4 Antimalarial drug combinations or single

Many studies have been conducted to find effective malaria treatments, but resistance to chloroquine and artemisinin has forced researchers to look for other strategies. One of the most applied methods has been to combine therapies to increase the individual therapies' efficiency in curing malaria.

Table 1 shows the common drugs used to treat each species of *Plasmodium* and their classification.

Table 1. Drugs and drug combinations authorized for human use against the different species of *Plasmodium*

Specie	Drug	Drug Classes
<i>P. vivax</i>	Chloroquine (World Health Organization, 2018)	4-aminoquinoline (Conrad & Rosenthal, 2019)
	Primaquine (Conrad & Rosenthal, 2019)	8-aminoquinoline (Milligan et al., 2019)
	Tafenoquine (Conrad & Rosenthal, 2019)	8-aminoquinoline (A. Rios et al., 2017)
	Cloroquine+Primaquine (S. Durand et al., 2018)	4-aminoquinoline (Conrad & Rosenthal, 2019), 8-aminoquinoline (Milligan et al., 2019)
	Artemisinin-based combination treatments (ACT) (World Health Organization, 2015)	Sesquiterpenic endoperoxide (M. Rodriguez, 2017), Folate antagonists (C. Rodriguez & Obrador, 2013)
<i>P. falciparum</i>	Artemisinin-based combination treatments (ACT) (World Health Organization, 2018)	Sesquiterpenic endoperoxide (M. Rodriguez, 2017), Folate antagonists (C. Rodriguez & Obrador, 2013)

	Quinine + clindamycin (Obonyo & Juma, 2012)	Quinoline (Shoemaker, 2002), Lincosamides (Perez & Morales, 2016)
	Chloroquine (World Health Organization, 2018)	4-aminoquinoline (Conrad & Rosenthal, 2019)
	Artesunate/amodiaquine (ASAQ) (Msellem et al., 2020)	Sesquiterpenic endoperoxide (M. Rodriguez, 2017)
	Mefloquine + artesunate (S. Durand et al., 2018)	Methanol quinolines (Giraldo & Blair, 2003), Sesquiterpenic endoperoxide (M. Rodriguez, 2017)
	Atovaquone-proguanil (Malarone) (R. Durand et al., 2008)	Quinone-folate antagonist combination (Ministerio de sanidad, 2016)
<i>P. ovale</i>	Primaquine (Conrad & Rosenthal, 2019)	8-aminoquinoline (Milligan et al., 2019)
	Tafenoquine (Conrad & Rosenthal, 2019)	8-aminoquinoline (A. Rios et al., 2017)
	Chloroquine (Lalloo, 2013)	4-aminoquinoline (Conrad & Rosenthal, 2019)
<i>P. malarie</i>	Chloroquine (World Health Organization, 2015)	4-aminoquinoline (Conrad & Rosenthal, 2019)
<i>P. knowlesi</i>	Chloroquine (World Health Organization, 2015)	4-aminoquinoline (Conrad & Rosenthal, 2019)

2.5 Derivatives of Chloroquine and Artemisinin

Chloroquine ($C_{18}H_{26}ClN_3$), by IUPAC nomenclature 4-N-(7-chloroquinolin-4-yl)-1-N,1-N-diethylpentane-1,4-diamine, is a 4-aminoquinolone drug (National Center for Biotechnology Information., 2021). Its molecular structure consists of a quinolone ring and its substituents chlorine and an amine group in the seventh and fourth positions, respectively (Aguiar et al., 2018). Chloroquine applications are in viruses, anti-inflammatory conditions, and cancer cells that cause the cell more sensitive to chemotherapy and radiotherapy due to the release of cellular degradation enzymes and the inhibition of transmembrane protein (Abdulkadir, 2019). The derivatives based on chloroquine as a template are SKM13 and SKM14. The difference between these two compounds and the original chloroquine is that CQ has the methyl group on the side chain, and their derivatives have phenylmethyl groups (derived from phenylalanine and α,β -unsaturated amide) instead of the methyl group. The difference between the products (SKM13 and SKM14) is α,β -unsaturated amide in SKM13 that is shorter than that in SKM14. Study on these derivatives suggest that SKM13 and SKM14 have enhanced antimalarial activity as they inhibit *P. berghei* (a *Plasmodium* infecting species of rodents) growth in blood and increase the survival rate from 40% to 100% (Yeo et al., 2017). Figure 3 shows the chloroquine structure.

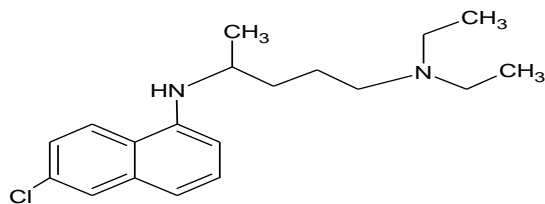


Figure 3. Chloroquine Structure (Made by Mishell Ortiz).

Artemisinin ($C_{15}H_{22}O_5$), with IUPAC name *1R,4S,5R,8S,9R,12S,13R*-1,5,9-trimethyl-11,14,15,16-tetraoxatetracyclo[10.3.1.0^{4,13}.0^{8,13}]hexadecan-10-one, is a sesquiterpene lactone (National Center for Biotechnology Information., 2021). Artemisinin applications include decreasing coccidial infection in chickens and treating other parasites such as *Schistosoma* spp., *Leishmania* spp., and *Toxoplasma* spp. (Pinheiro et al., 2018). The derivatives of artemisinin are Dihydroartemisin, Artesunate, and Artemether. These drugs act in the parasite vacuole by converting heme into nontoxic hemozoin (Chassaingne, 2001). These drugs are blood schizonticides that operate on gametocytes that reduce the propagation of resistant forms and prevent the transmission to other hosts (Pinheiro et al., 2018). Figure 4. presents the structure of artemisinin.

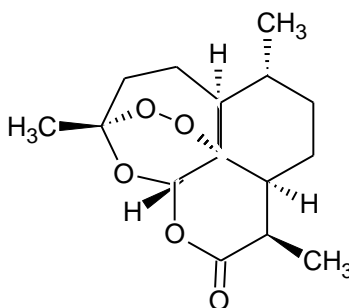


Figure 4. Artemisinin Structure (Made by Mishell Ortiz).

2.6 Mode of action of Chloroquine and Artemisinin

The parasite of malaria acquires a heme group, which is toxic to cells, from host hemoglobin in the intraerythrocytic stages. Also, the heme is converted to hematin, and through dimerization occurs in a β -hematin form. The β -hematin form is still toxic, so the parasite converts it into an insoluble crystalline form called hemozoin through a biocrystallization process. The chloroquine mode of action involves the parasitophorous vacuole because chloroquine is trapped inside the vacuole and prevents the biocrystallization of β -hematin. This action occurs due to the parasite vacuole's acidic nature, which allows the chloroquine to get in the impermeable membrane doubly protonated. The parasite's death is caused by the complex formed by chloroquine with free heme, which produces an accumulation of heme (Lawrenson et al., 2018). Also, this drug interferes with the biosynthesis of nucleic acids (National Center for Biotechnology Information, 2021).

In Figure 5, the immunological mechanism mediated by chloroquine in the host's immune response is summarized. The antigen presentation by the antigen presentation cell (APC) activates the T cell as are macrophages and dendrite cells release pro-inflammatory cytokines (Schrezenmeier & Dörner, 2020). Chloroquine can inhibit Toll-like receptor (TLR) signaling, especially TLR7 and TLR9, due to changes in endosomal pH or the binding of

chloroquine with nucleic acids. Also, TLR signals stimulate cytokine production, and chloroquine might inhibit cytokine production through the blocking of TLR pathways. Subsequently, chloroquine reduces the production of anti-inflammatory cytokines such as IL-1, IL-6, TNF, and IFN γ by T cells. Finally, this drug also inhibits MHC class II antigen presentation to T cells and the co-stimulatory molecule expression, CD154 (Schrezenmeier & Dörner, 2020).

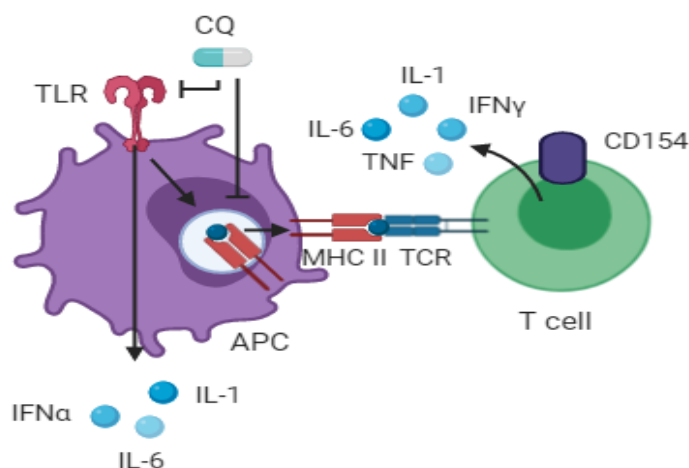


Figure 5. The cellular immune response of chloroquine action (Figure made by Mishell Ortiz).

Artemisinin interacts with the parasite's heme and the intraparasitic heme or iron that help activate artemisinin into toxic free radicals that produce the parasite's kill inhibition degradation of hemozoin biosynthesis (Meshnick, 2002). The mode of action of artemisinin starts with the activation of reactive oxygen species. The essential part of artemisinin's antimalarial activity is the endoperoxide bridge in the trioxane pharmacophore. The bioactivity is due to replacing one peroxidic oxygen with a carbon (Cui & Su, 2009). The formation of free radicals damages the specific intracellular targets via alkylation (Meshnick, 2002). The artemisinin inhibits sarcoplasmic reticulum Ca²⁺-ATPase activity of malaria parasites (Gopalakrishnan & Kumar, 2015). The mechanism of action in the derivatives of Artemisinin like Artemether has been seen in the interference with mitochondrial electron transport, plasmodial transport protein, and the production of free radicals to reduce blood antioxidants and glutathione (Pinheiro et al., 2018). The other derivative, Artesunate, involves direct DNA damage killing the parasite (Gopalakrishnan & Kumar, 2015).

2.7 Antimalarial resistance

Antimalarial drugs have lost their effectiveness due to the bad administration and prolonged use of the drugs, which has led to the development of drug resistance. The main specific causes of antimalarial drug resistance are incorrect dosing, drug absorption, unusual pharmacokinetics, the mutation of the parasite, cross-resistance, vector and environment, host immunity, the low transmission of malaria. Another cause of resistance is treatment failure like try to resolve clinical symptoms, despite using correct doses of the antimalarial drug (World Health Organization, 2015;Sinha et al., 2014) The spread of drug resistance on a large scale is a problem for the fight against the disease and has spurred the research into the creation of a new vaccine that can limit the transmission of the parasite (Noronha et al., 2020).

The resistance generated by *Plasmodium falciparum* against chloroquine is due to a mutation called PfCRT (*Plasmodium falciparum* chloroquine resistance) that occurred at position 76 (K76T) (Noronha et al., 2020). This mechanism is due to the parasite's resistant strains against chloroquine having a neutral threonine residue in lieu of the PfCRT protein's positively charged lysine moiety (Lawrenson et al., 2018).

Artemisinin resistance is caused by the Kelch protein, specifically by point mutations in the phosphatidylinositol-3-kinase gene (Pfk13 or K13) of *P. falciparum* (Noronha et al., 2020). The mutation in K13 has been associated with endoplasmic reticulum of the parasite and improper protein folding (Bhattacharjee et al., 2018). Furthermore, this gene is near to the parasite's food vacuole that is responsible for digesting material endocytosed from the red blood cells of the host. This digestion produces heme, and their interaction with artemisinin allows the death of the parasite (York, 2020). The point mutations C5080Y, Y493H, and R539T in K13 correlate with the prevalence of resistance to artemisinin (Fairhurst & Dondorp, 2016).

Table 2 shows some antimalarial drugs (chloroquine, amodiaquine, piperaquine, quinine, mefloquine, artemisinin, artemether, artesunate, and primaquine) reported by Africa with their respective resistance polymorphisms (Conrad & Rosenthal, 2019; Gendrot et al., 2017; Conrad et al., 2019).

Table 2. Some antimalarial drugs with their respective resistance polymorphisms

Antimalarial drugs	Polymorphism that involve resistance	References
Chloroquine	Pfcr1 76Thr; pfmdr1 86Tyr and 1246Tyr	(Conrad & Rosenthal, 2019)
Amodiaquine	Same mutations as chloroquine	(Conrad & Rosenthal, 2019)
Piperaquine	Increased plasmepsin-2 copy number; pfcr1 SNPs	(Conrad & Rosenthal, 2019)
Quinine	SNPs in pfmdr1, pfmdr6	(Gendrot et al., 2017)
Mefloquine	More pfmdr1 copy number	(Conrad & Rosenthal, 2019)
Artemisin	K13PD mutations	(Conrad et al., 2019)
Artemether	K13PD mutations	(Conrad & Rosenthal, 2019)
Artesunate	K13PD mutations	(Conrad & Rosenthal, 2019)
Primaquine	Resistance not documented	(Conrad & Rosenthal, 2019)

2.8 Humoral response in malaria

The response generated by antibody-mediated exposure to antigens is called the humoral response. Exposure of a vertebrate immune system to an antigen (virus, bacteria, parasite, or fungus) produces a humoral response. The humoral response implicate to B cells' activity with the antigen to differentiate into plasma cells and secrete antibodies. Subsequently, the antibody binds to the antigen to activate the immune system and the

different lympho- and leucocytes (Kindt et al., 2007). The malaria parasite has many antigenic proteins (for example, GLURP, MSP3, and MSP1-19, AMA-1) on its surface and on the apical membrane system, which activate the host's immune system (Diarra et al., 2012).

The humoral response was evaluated in Gambian children with malaria who were treated with chloroquine in 28-day trials. The recovery of the children focused on the absence of malaria and parasitemia. Therefore, children's plasma samples were analyzed using ELISA to determine IgG against Apical Membrane Antigen 1 (AMA-1), Merozoite Surface Protein 1 to 19 fragment of the C terminal protein (MSP1-19) antigens and MSP-1 antigenic variants with double and triple substitutions. IgG titers to MSP1-19 and the triple variant were the highest in plasma samples from children recovered after seven treatment days. Besides, children who presented parasitemia on 14 or 28 days showed an age-independent relationship between the parasite density and IgG concentration for MSP-19 and the triple variant (Pinder et al., 2006).

In another study, the humoral response of IgG, IgM, and sub-classes of IgG (IgG1, IgG2, IgG3, IgG4) between MSP3, MSP1-19, and Glutamate rich *Plasmodium falciparum* (GLURP) antigens was determined through the indirect ELISA test. The study was carried out with 248 children between 0, 5, and 15 years old; all of them had AA hemoglobin genotype, which means that this blood group presents a malaria infection relation. The efficacy of each drug's treatments (chloroquine and sulphadoxine/pyrimethamine (SP) in the treatment of *Plasmodium falciparum*) were verified. The effectiveness of chloroquine was evidenced with the levels of IgG, IgG1, and IgG2 against MSP3, while for the GLURP antigen, there was a strong association with IgG and IgM. The efficacy of SP treatment's was for IgG3 against MSP3, none of the other antigens showed a relationship between efficacy and antibody levels. The relationship between age and level of antibodies with the antigens was also studied. The results showed that the MSP3 and GLURP antigens presented a more significant amount of antibodies in older children than 15-year-old than in younger children (Diarra et al., 2012).

2.9 Cross-reactivity assay in the malaria evaluation

Cross-reactivity is defined as the interaction of antibodies with an unrelated antigen. This occurs if two different antigens share an identical or similar epitope (Kindt et al., 2007).

There are reports in the literature that evaluate the antibody response using the ELISA test with anti-malarial drugs. A cross-reactivity study of chloroquine with amino quinolines and other malarial drugs was performed to verify specificity. The study developed a monoclonal antibody against CQ. ELISA confirmed chloroquine's specificity towards the monoclonal antibody (mAb), and this mAb recognized chloroquine as its antigen. In contrast, the other compounds (mefloquine, hydroxyl-chloroquine, quinine, pyrimethamine, quinine trimethoprim, sulphamethoxazole, and sulphadoxine) were not recognized by mAb, and there was no cross-reactivity (Khalil et al., 2011).

In another cross-reactivity study with drugs, piperazine (PPQ) had cross-reactivity with artemisinin derivatives and other antimalarial drugs. The experiment was carried out with a monoclonal antibody against piperazine in five weeks old female BALB/c mice. Indirect ELISA was performed to evaluate the cross-reactivity between drugs. The results suggested that piperazine reacted 100% with its antigen as expected and exhibited less cross-reactivity with amodiaquine, chloroquine, and hydroxychloroquine sulfate. While for the other drugs as antigens do not present a cross-reactivity with artemisinin,

dihydroartemisinin, artesunate, artemether, lumefantrine and mefloquine. This cross-reactivity can be explained by the presence of 7-chloro-4- (piperazin-1-yl) quinolone in the chemical structure of PPQ with other 4-aminoquinoline drugs (Ning et al., 2019).

Another experiment demonstrates the cross-reactivity of artemisinin and other related analytes. This experiment was done using monoclonal antibodies (3HH2) in female BALB/c mice, seven weeks old. The indirect ELISA test was performed to evaluate the cross-reactivity of the antigens. This work showed that mAb artemisin reacted with the artesunate antigen, then with its antigen, and dihydroartemisinin. While for the drugs deoxyartemisin, arteannuin B and artemisinic acid did not present cross-reactivity with mAb (Su-ping et al., 2009).

Finally, another study showed the cross-reactivity study by competitive ELISA of anti-artesunate with other antimalarial drugs was reported. The mentioned research reported the polyclonal antibodies from mice immunized with artesunate were used in the ELISA test. The cross-reactivity of artesunate recognizes its antigen and also artemisinin, and dihydroartemisinin. The other antimalarial drugs (quinine, chloroquine, primaquine, mefloquine, amodiaquine, pyrimethamine, and sulfadiazine) do not present recognition by polyclonal antibodies (Mitsui, 2016).

3.0 Tetrahydro-2h-1,3,5-thiadiazine-2-thione (THTT) derivatives

THTT (tetrahydro-2H-1,3,5-thiadiazine-2-thione THTT) have many drug research applications, thanks to high lipid solubility, enzymatic rate of hydrolysis, and stability in a simulated gastric fluid that facilitates stomach absorption. THTT derivatives have antiprotozoal, antibacterial, antifungal, anthelmintic, and tuberculostatic properties evaluated in previous studies. In addition, THTTs have been used for arteriosclerosis treatment and antiepileptic prodrugs (Rodríguez et al., 2012).

The protozoan properties of THTT derivatives have been reported since 1999, in studies of *Trichomonas vaginalis* and *Trypanosoma cruzi*. In 2000, there was a report of THTT related to anticancer properties (Bermello et al., 2011). In 2006, a study evaluated the *in vitro* antiprotozoal activity of alkyl-linked bis tetrahydro-(2H)-1,3,5-thiadiazine-2-thione (bis-THTT) belonging to series I and II on *Leishmania donovani*, *Trypanosoma brucei rhodesiense* and *Plasmodium falciparum*. The results obtained in these experiments show efficacy only in *T. b. rhodesiense* (Coro et al., 2006).

Figure 6 shows the chemical structure of compounds derived from alkyl-linked bis-(2-thioxo-[1,3,5] thiadiazinan-3-yl) carboxylic acids.

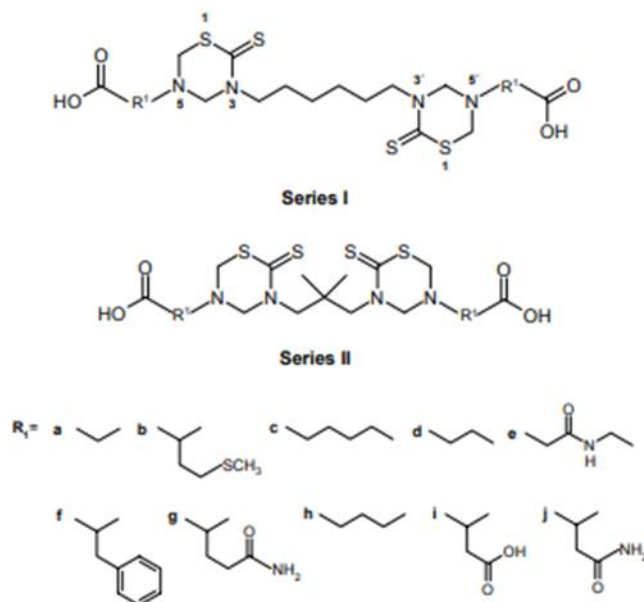


Figure 6. Chemical structure of compounds derived from alkyl-linked bis-(2-thio- [1,3,5]thiadiazinan-3-yl) carboxylic acids (From Coro et al., 2006).

Finally, in 2008, an experiment demonstrated the antiprotozoal evaluation of new N4-(Benzyl) spermidyl-linked bis (1,3,5-thiadiazinane-2-thiones) on *L. donovani*, *T. cruzi*, *T. b. rhodesiense* STIB900, and *P. falciparum* 3D7 strains. The experiment results showed an antiprotozoal activity only against *T. cruzi* and *L. donovani* (Coro et al., 2008).

3.1 Chemical structure of bis-tetrahydro-2H-1,3,5-thiadiazine-2-thione (THTT) and its origin

The chemical structure of bis-tetrahydro-2H-1,3,5-thiadiazine-2-thione (bis-THTT) consists of two rings as the central core, connected via their N-3 atom by a linear aliphatic backbone and bearing carboxyalkyl or alkyl residues at N-5. Figure 7 shows the synthetic pathway for obtaining bis-THTT starts using diamines. The first step consists of diamine's reaction with carbon disulfide and potassium hydroxide to get bis-dithiocarbamate salt. The amounts of reagents were duplicated in the following step. The second step is adding the formaldehyde and the desired amino acid to obtain the corresponding bis-THTT (Bermello et al., 2011).

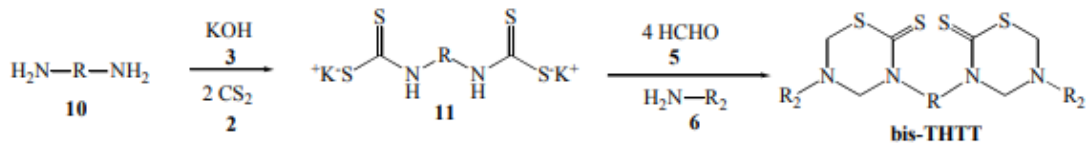


Figure 7. Procedure for obtaining bis-THTT (From Bermello et al., 2011)

2. PROBLEM STATEMENT

Chloroquine and other antimalarial drugs have been losing their biological activity due to increased drug resistance to the mentioned disease. Therefore, it is crucial to research

new drugs to find viable candidates that can eradicate malaria disease. In previous studies (Coro et al., 2005, 2008), the antiparasitic activity against protozoa of the compounds derived from bis-THTT have been shown to have antiprotozoal activity to *Trypanosoma cruzi*, *T. vaginalis*, *T. b. rhodesiense* and *Leishmania donovani*. Hence, these compounds could have antimalarial activity, opening a new venue for the search of compounds capable of overcoming resistance to the currently used drugs.

3. HYPOTHESIS

The compounds' antimalarial activity was previously evaluated *in vivo* in rodent systems with two murine *Plasmodium* strains. They were *P. yoelii* 17XL and *P. berghei* ANKA strains, showing some antimalarial activity in two compounds JH2 and JH4 for *P. yoelii*. For *P.berghei* with the JH5 and JH6 compounds, although they did not equal the activity of Chloroquine (Loachamin et al., 2019). Therefore, in this study, we expect to find cross-reactivity between compounds with hyperimmune sera from female BALB/c mice by indirect ELISA assay, based on identifying the compounds' chemical structures by recognizing the polyclonal antibodies. Hoping to obtain recognition between the most similar chemical structures and relate them to the previously evaluated antimalarial activity.

4. OBJECTIVES

4.1 General Objective

To carry out the chemical characterization of six bis-THTT by its melting point and using spectroscopy techniques such as FT-IR, UV/Vis, and chromatographic (UHPLC) procedures. At the same time, to evaluate the ability of the six bis-THTT to develop humoral response with hyperimmune sera obtained from BALB/c mice immunized with the compounds by indirect ELISA assay and cross-reactivity of each compound.

4.2 Specific Objectives

- To chemically characterized the six compounds bis-THTT through its melting point (mp), Infrared spectroscopy (FT-IR), and Ultraviolet/visible spectroscopy (UV/Vis).
- To determine the bis-THTT purities using Ultra-High Performance Liquid Chromatography (UHPLC).
- To evaluate the humoral response of the compounds derived from bis-THTT with indirect ELISA test using hyper-immune sera from immunized BALB/c mice as primary antibodies.
- To determine the compounds' cross-reaction by recognizing the indirect ELISA assay's polyclonal antibodies, using the experimental compounds and chloroquine as antigens.
- This is based on the previous objective results to evaluate cross-reactivity using two antigens combined in an indirect ELISA assay.

5. MATERIALS AND METHODS

5.1 Compounds derived from bis-THTT

This study was evaluated the following six THTTs labeled JH1, JH2, JH3, JH4, JH5, JH6 (Figures 8, 9, 10, 11, 12, and 13), which are derivatives of bis-tetrahydro-(2H)-1,3,5-thiadiazine-2-thione. Chloroquine was used as the anti-malaria drug-positive control. These

compounds were derived from bis-THTT were previously synthesized in the Organic Synthesis Laboratory from the University of Havana and kindly donated for this research by Dr. Hortensia Rodriguez, Department of Chemistry, Yachay Tech University.

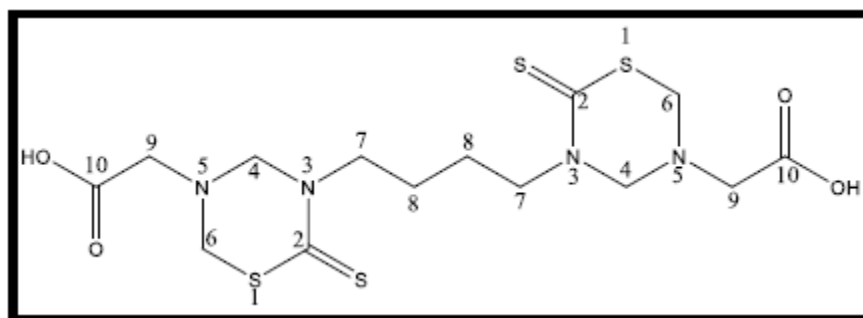


Figure 8. Chemical structure of JH1 compound, 2-(5-{6-[5-(Carboxymethyl)-2-thioxo-1,3,5-thiadiazinan-3-yl]butyl}-6-thioxo-1,3,5-thiadiazinan-3-yl)-ethanoic acid.

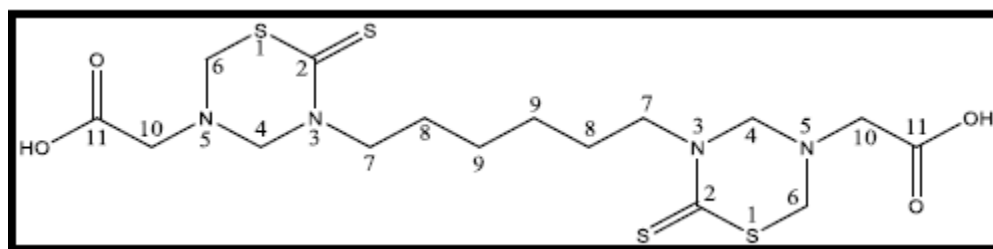


Figure 9. Chemical structure of JH2 compound, 2-(5-{6-[5-(carboxymethyl)-2-thioxo-1,3,5-thiadiazinan-3-yl]hexyl}-6-thioxo-1,3,5-thiadiazinan-3-yl)-ethanoic acid.

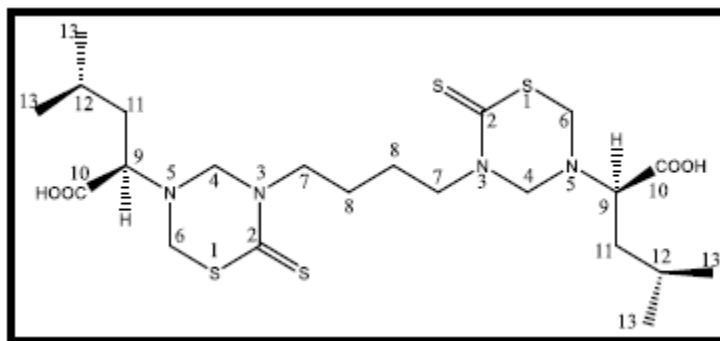


Figure 10. Chemical structure of JH3 compound, (2S)-2-[5-(6-{5-[(1S)-1-carboxy-3-methylbutyl]-2-thioxo-1,3,5-thiadiazin-3-yl}butyl)-6-thioxo-1,3,5-thiadiazin-3-yl]-4-methylpentanoic acid.

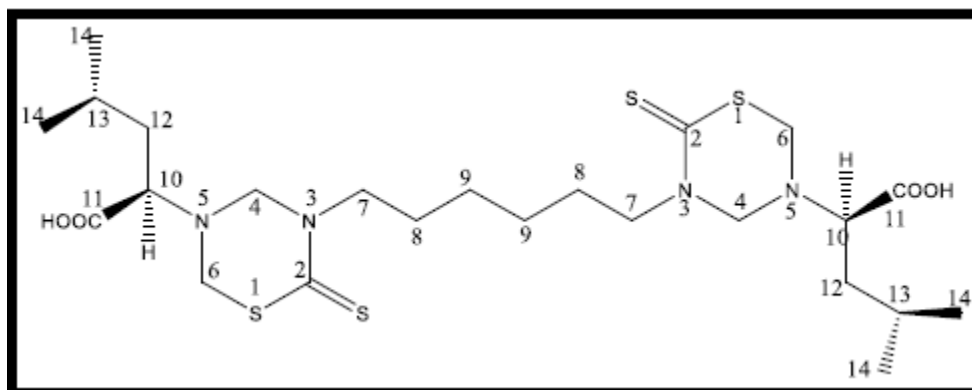


Figure 11. Chemical structure of JH4 compound, (2S)-2-[5-(6-{5-[(1S)-1-carboxy-3-methylbutyl]-2-thioxo-1,3,5-thiadiazinan-3-yl}hexyl)-6-thioxo-1,3,5-thiadiazinan-3-yl]-4-methylpentanoic acid.

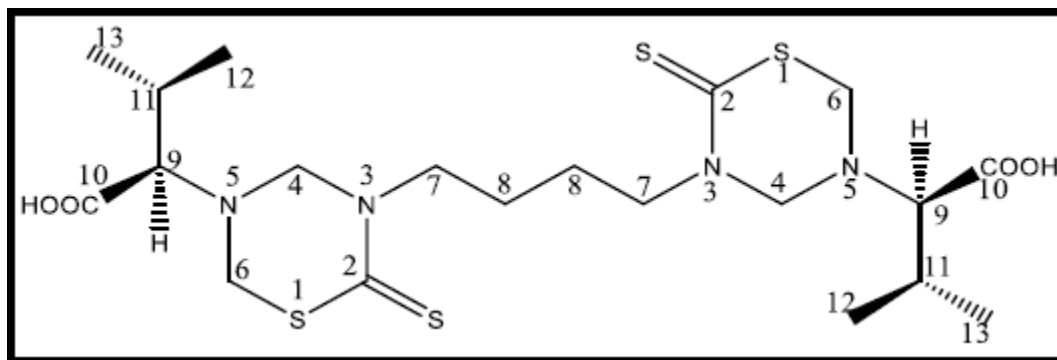


Figure 12. Chemical structure of JH5 compound, 2-(5-{6-[5-(1-carboxy-1-methylpropyl)-2-thioxo-1,3,5-thiadiazinan-3-yl]butyl}-6-thioxo-1,3,5-thiadiazin-3-yl)-3-methylbutanoic acid.

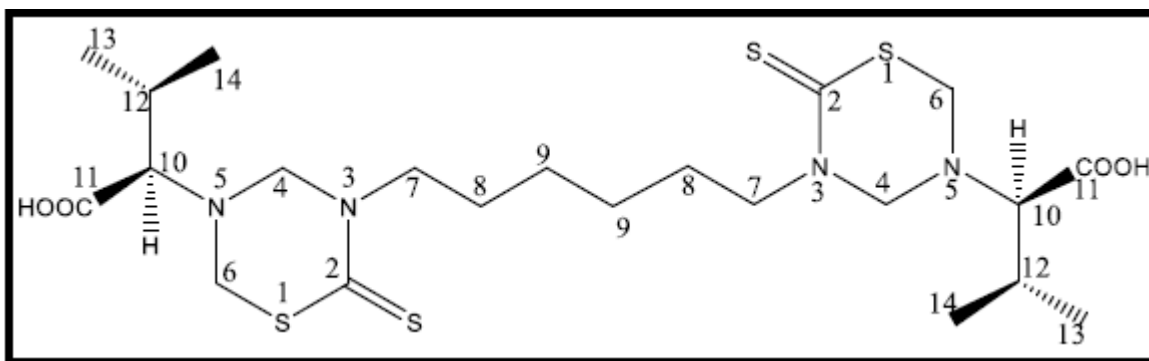


Figure 13. Chemical structure of JH6 compound, 2-(5-{6-[5-(1-carboxy-1-methylpropyl)-2-thioxo-1,3,5-thiadiazinan-3-yl]hexyl}-6-thioxo-1,3,5-thiadiazin-3-yl)-3-methylbutanoic acid.

All THTTs were diluted in distilled water to an initial concentration of 100 mg/. Dimethyl Sulfoxide (DMSO) was added to those samples with aqueous dilution problems. See section 6.2.1.

5.2 Melting point

The melting point was performed on an Electrothermal Melting Point Apparatus. The solid compounds (JH1, JH2, JH3, JH4, JH5, and JH6) were introduced in a capillary tube and then placed in Electrothermal apparatus. The ramp rate used was two degrees per minute until 90°C, and finally reaches each melting point with 0.2 celsius degree per minute. The state's change inside the capillary tube is observed, and the apparatus's temperature is noted.

5.3 Fourier-transform infrared spectroscopy

FT-IR spectrometry was performed in a Cary 630 Agilent FTIR spectrometer. The analysis was done by the Total Reflection Attenuated (ATR) method in a wavelength range of 5100-600 cm^{-1} . It is important to clean the diamond with Ethanol before using the FT-IR apparatus, then put a bit solid sample for each compound (JH1, JH2, JH3, JH4, JH5, and JH6) on top of a crystal and tighten down the clamp so that the FT-IR radiation can interact with the sample and the spectrum could be generated.

5.4 UHPLC and UV/Vis

The system used for UHPLC was Dionex UltiMate 3000 with a UV/Vis detector at wavelength 254 nm. Also, this analysis was carried out using the software Chromeleon. The preparation of compounds started with the measure of 1 mg of each compound, and then, each compound was diluted with 500 μl of DMSO and 500 μl of type 1 water. The injection volume was 20 μl , the run was in gradient, and the run flow was 1 ml/min. Gradient elution was performed at room temperature with type 1 water and Acetonitrile, in the following order for Acetonitrile: 0% until 0-1 min, 70% in 1-2 min, 100% in 2-8 min, and 0% in 8-10 min.

5.5 Indirect ELISA test using the experimental compounds as antigens

Voller's protocol (1976, 1980) was followed to obtain the indirect ELISA test's optimal conditions.

1. ELISA plates (96-well Nunc) were sensitized, with 100 μl of the soluble compounds in each well with 10 $\mu\text{g}/\text{ml}$ of concentration and diluted in carbonate-bicarbonate buffer at pH 9.6 (0.5 M Na_2CO_3 and 0.35 M NaHCO_3). The plates were incubated in a humid chamber at a temperature of 4 °C overnight. After, they were washed (3 times for 3 minutes each time) using 200 μl per well of phosphate-buffered saline and Tween 20 at 0.005% (PBS/T).
2. The wells were blocked with 100 μl of Bovine Serum Albumin (BSA) at 3%, diluted in PBS buffer. Then, the plates were incubated in a humid chamber at 37 °C for 1 hour. After this time, the plates were washed (3 times for 3 minutes each time) with PBS/T solution.
3. The distribution of the antigen and primer antibodies are shown in the table 3. In the wells were added 100 μl of PBS as the negative control, and hyper-immune sera of immunized BALB/c mice with the antigens (CQ, JH1, JH2, JH3, JH4, JH5 and JH6), diluted in PBS Buffer at 1:200. See distribution in tables 3, 4, 5 and 6. Subsequently, the plates were incubated in a humid chamber at 37 °C for 1 hour. After, the plates were washed (3 times for 3 minutes each time) with PBS/T solution.
4. The next step was to add the conjugate. Each well 100 μl of the conjugate, anti-mouse/IgG peroxidase antibody produced by goat conjugated to the peroxidase enzyme (HRP-peroxidase Horseradish; Sigma) in 1:1000 of dilution, were added in PBS Buffer. After, the plates were incubated in a humid chamber at 37 °C for 1 hour. the plates' washing was carried out (3 times for 3 min each time) with PBS/T solution.

- Finally, to develop the chromogenic enzyme reaction, 100 μ l of the chromogen ABTS (2,2'-azino-bis (3-ethylbenzthiazoline-6-sulfuric acid, Sigma) as substrate and added 0.05% of H₂O₂, in 100 μ l per well. Then, plates remained in the dark for 60 minutes at room temperature, and they were read at 405 nm. The readings were made every 5 minutes to determine the optimal reading time for each compound.

Table 3. Distribution of antigens and sera in the ELISA plate 1

		PBS	PIS	CQS	JH1S	JH2S	JH3S	JH4S	JH5S	JH6S				
		1	2	3	4	5	6	7	8	9	10	11	12	
JH1	10 μ g/ml	A												
		B												
		C												
		D												
JH2	10 μ g/ml	E												
		F												
		G												
		H												

The rest of the experimental compounds followed the same distribution of table 3.

5.6 Indirect ELISA test with two combinations of antigens

The two antigens that showed similar recognition by the hype-immune sera were chosen to combine as antigens in these indirect ELISA tests based on the cross-reactivity reactions obtained in the previous indirect ELISA tests.

This indirect ELISA experiment follows the same conditions of protocol indicated in section 5.5. The only difference is the antigens used because, in this experiment, the combination of two antigens was used (CQ+JH1, CQ+JH4, JH1+JH3, JH1+JH4, JH2+JH3, JH2+JH4, JH4+JH3, JH5+JH4, JH5+JH6, JH6+JH4, JH6+JH3). The combination of antigens was 200 μ l of antigen one plus 200 μ l of antigen two at ten μ g/ml of concentration and diluted in carbonate-bicarbonate buffer at pH 9.6. The distribution of the combination of antigens is shown in table 4.

Table 4. Distribution of combination of antigens in the ELISA plate 1

		PBS	PIS	CQS	JH1S	JH2S	JH3S	JH4S	JH5S	JH6S				
		1	2	3	4	5	6	7	8	9	10	11	12	
CQ+JH4	10 μ g/ml	A												
		B												
		C												
		D												
JH1+JH3	10 μ g/ml	E												
		F												
		G												

* Melting points reported in (Coro et al., 2005).

According to organic compounds features, all analyzed bis-THTT showed lower mp values, with melting ranges of two or three degrees Celsius. The mp of the two bis-THTT JH2, and JH4, were closer to those previously reported (Coro et al., 2005).

6.1.2 FT-IR of bis-tetrahydro-2(1H)-thiadiazine-2-thiones (JH1-JH6) in experimental compound

The THTT ring formation was confirmed by FT-IR spectroscopy because this technique allows us to identify functional groups (Pretsch et al., 2000). As was expected, the FT-IR spectra of the six bis-THTT were so similar. Figures 14 and 15 showed, as an example, selected IR spectra for JH1 and JH2. The presence of the characteristic band of the carbonyl ($\nu\text{C}=\text{O}$, blue) and thiocarbonyl ($\nu\text{C}=\text{S}$, red) groups around 1720 cm^{-1} and 1480 cm^{-1} , respectively, but also the broad characteristic band of hydroxyl (OH) at around 3000 cm^{-1} (νOH , orange) was confirmed in the IR spectra of all JHs.

As additional signals, it is possible to point those corresponding to C-H stretching ($\nu\text{C-H}$) of the aliphatic chain that joins both rings through the nitrogen at the positions three around 2800 cm^{-1} , and the band around 1338 cm^{-1} corresponding to C-H bending of methylenes ($\delta\text{C-H}$). A strong signal at 1125 cm^{-1} corresponding to C-O stretching ($\nu\text{C-O}$) around 1125 cm^{-1} was also observed.

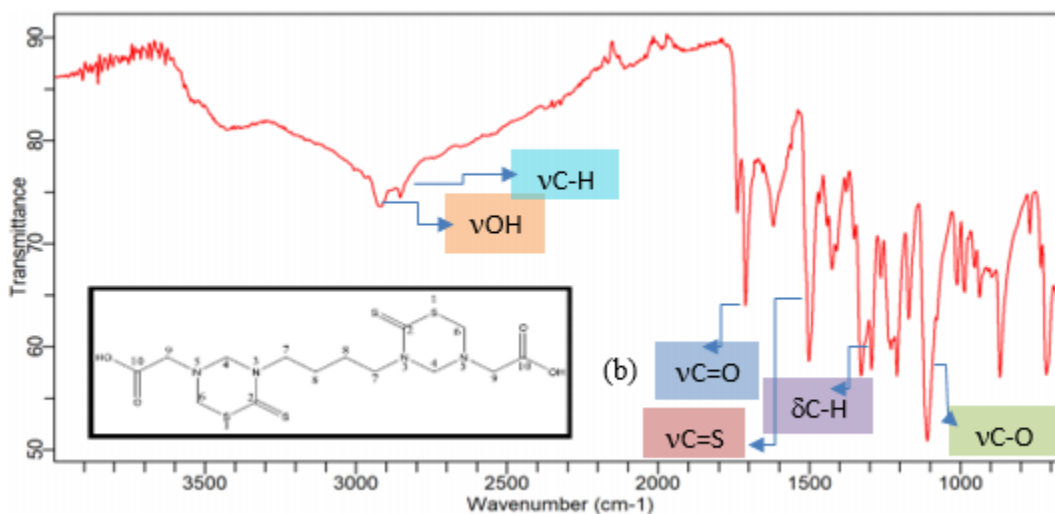


Figure 14. FT-IR absorption spectra of JH1 compound, 2-(5-{6-[5-(Carboxymethyl)-2-thioxo-1,3,5-thiadiazinan-3-yl]butyl}-6-thioxo-1,3,5-thiadiazinan-3-yl)-ethanico acid (a). On the X-axis are represented the wavenumber (cm^{-1}) vs. transmittance on the Y-axis.

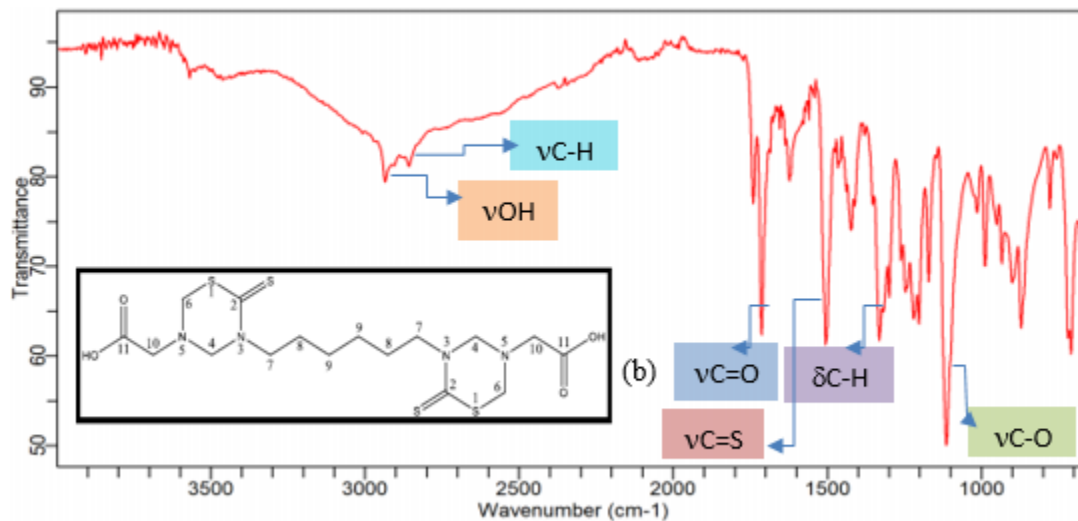


Figure 15. FT-IR absorption spectra of JH2 compound, 2- (5- {6- [5- (carboxymethyl) -2-thioxo 1,3,5-thiadiazinan-3-yl] hexyl} -6-thioxo 1,3,5-thiadiazinan-3-yl) ethanoic acid (b). On the X-axis are represented the wavenumber (cm^{-1}) vs. transmittance on the Y-axis.

Infrared spectra obtained for the other compounds are shown in the corresponding annexes (Annex 1, Annex 2, Annex 3, and Annex 4).

6.1.3 UV/Vis spectroscopy of bis-tetrahydro-2(1H)-thiadiazine-2-thiones (JH1-JH6)

The principle of UV/Vis spectroscopy is based on the absorption of ultraviolet and visible light by chemical compounds, which results in the spectrum. UV/Vis spectroscopy is currently only marginally relevant to structure elucidation but would be usefully applied to UV/Vis detectors like those used in HPLC and UHPLC chromatographic techniques.

All analyzed compounds showed two characteristic bands in the UV spectra, near 290 and 250 nm (Figure 16 and 17). The intense band at 290 nm was related to $n-\pi^*$ transition of the thione group. This assignment has been confirmed by previous studies, which showed that the mentioned signal disappears when the thiadiazine undergoes a ring cleavage (Ochoa et al., 1999). The less intense band near 250 nm would be assigned to electronic transition corresponding to the carbonyl's groups present in each molecule.

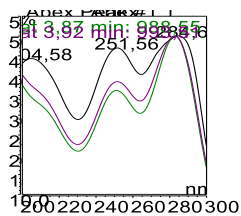


Figure 16. UV/Vis absorption spectra of JH1 compound, 2-(5-{6-[5-(Carboxymethyl)-2-thioxo-1,3,5-thiadiazinan-3-yl]butyl}-6-thioxo-1,3,5-thiadiazinan-3-yl)-ethanoic acid. On the X-axis are represented the wavelength (nm) vs. absorbance on the Y-axis.

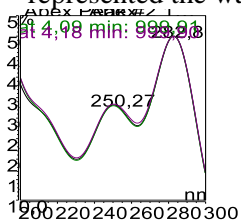


Figure 17. UV/Vis absorption spectra of JH2 compound, 2-(5-{6-[5-(carboxymethyl)-2-thioxo-1,3,5-thiadiazinan-3-yl]hexyl}-6-thioxo-1,3,5-thiadiazinan-3-yl)-ethanoic acid. On the X-axis are represented the wavelength (nm) vs. absorbance on the Y-axis.

The UV/Vis absorption spectra of compounds JH3, JH4, JH5, and JH6 are shown in the corresponding annexes (Annex 5, Annex 6, Annex 7, and Annex 8).

6.1.4 UHPLC of bis-tetrahydro-2(1H)-thiadiazine-2-thiones (JH1-JH6)

The Ultra-High-Performance Liquid Chromatography (UHPLC) is a technique to separate the components of a mixture and establish the purity of the compounds. All bis-THTT were analyzed using UHPLC equipment. The profiles for JH1, JH2, JH4, and JH6 (Figures 18, 19, 21, and 23) showed acceptable purities between 70% to 94 %. However, UHPLC profiles for JH3 and JH5 (Figures 20 and 22) exhibited a complicated chromatogram where the signal corresponding to the bis-THTT derivative is not clear. For that reason, recrystallization of JH3 and JH5 was carried out to achieve a better purity degree. Unfortunately, chromatograms could not be repeated for recrystallized compounds.

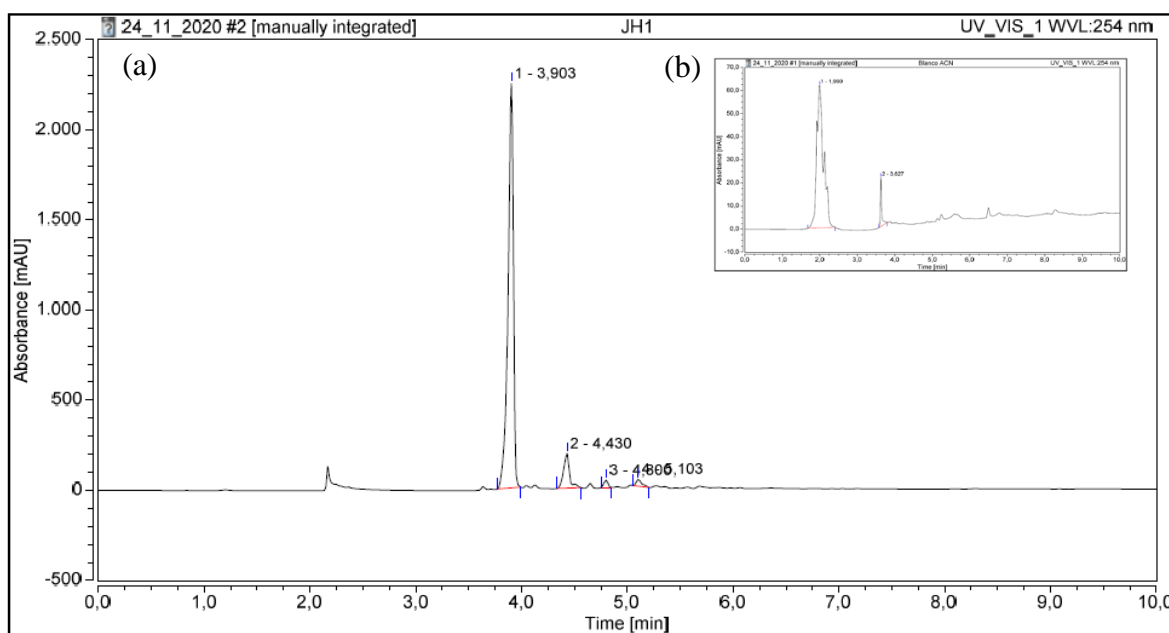


Figure 18. (a)UHPLC profile of JH1 compound, 2-(5-{6-[5-(Carboxymethyl)-2-thioxo-1,3,5-thiadiazinan-3-yl]butyl}-6-thioxo-1,3,5-thiadiazinan-3-yl)-ethanico acid. (b)UHPLC profile of acetonitrile blank

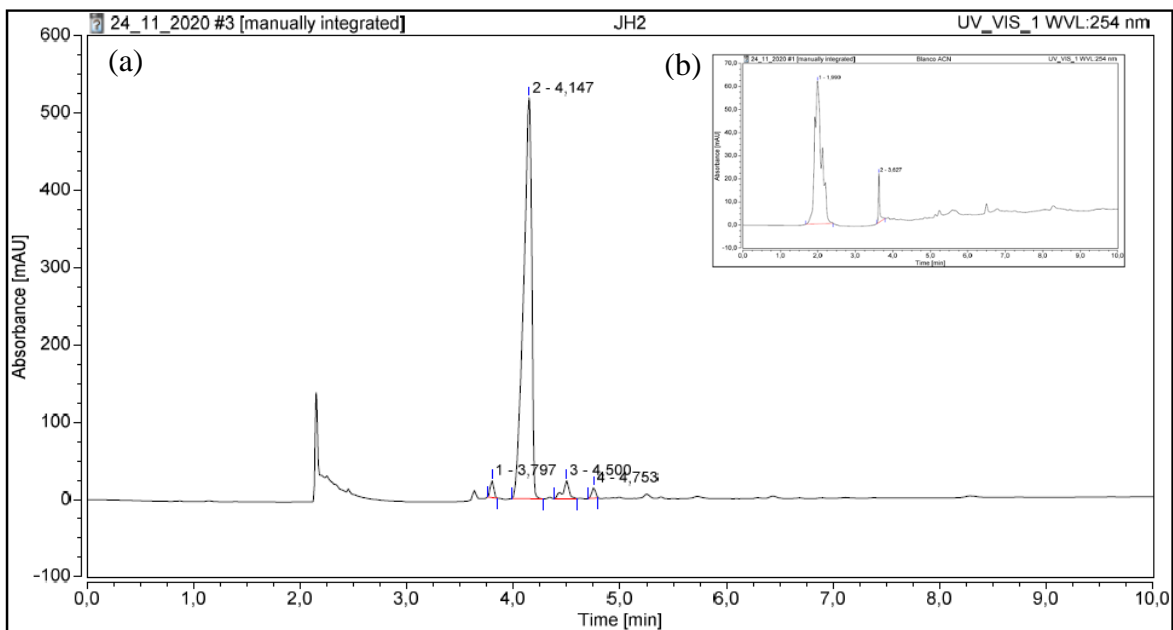


Figure 19. (a)UHPLC profile of JH2 compound, 2- (5- {6- [5- (carboxymethyl) -2-thioxo 1,3,5-thiadiazinan-3-yl] hexyl} -6-thioxo 1,3,5-thiadiazinan-3-yl) ethanoic acid. (b)UHPLC profile of acetonitrile blank

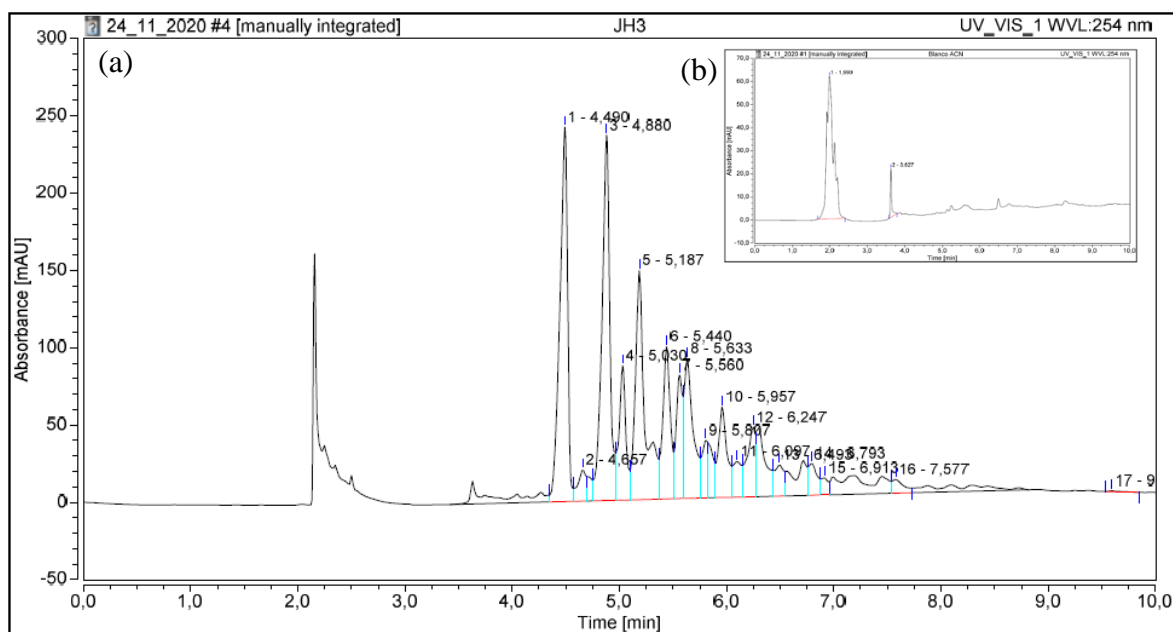


Figure 20. (a)UHPLC profile of JH3 compound, (2S)-2-[5-(6-{5-[(1S)-1-carboxy-3-methylbutyl]-2-thioxo-1,3,5 thiadiazin-3-yl}butyl)-6-thioxo-1,3,5-thiadiazinan-3-yl]-4 methylpentanoic acid. (b)UHPLC profile of acetonitrile blank

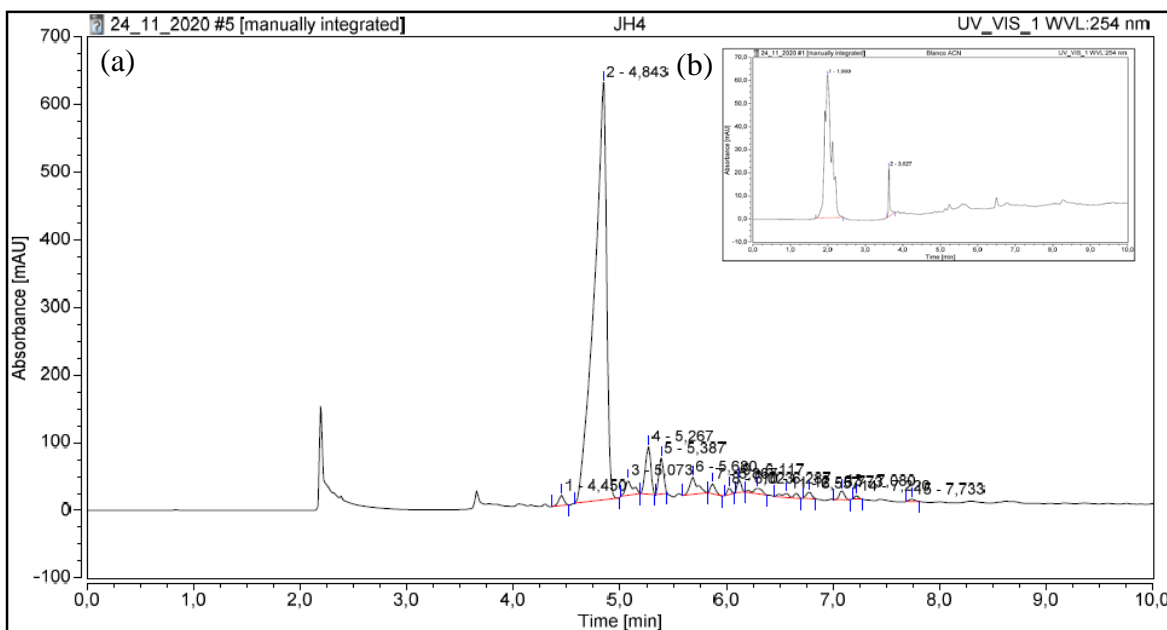


Figure 21. (a)UHPLC profile of JH4 compound, (2S)-2-[5-(6-{5-[(1S)-1-carboxy-3-methylbutyl]-2-thioxo-1,3,5-thiadiazinan-3-yl}hexyl)-6-thioxo-1,3,5-thiadiazinan-3-yl]-4-methylpentanoic acid. (b)UHPLC profile of acetonitrile blank

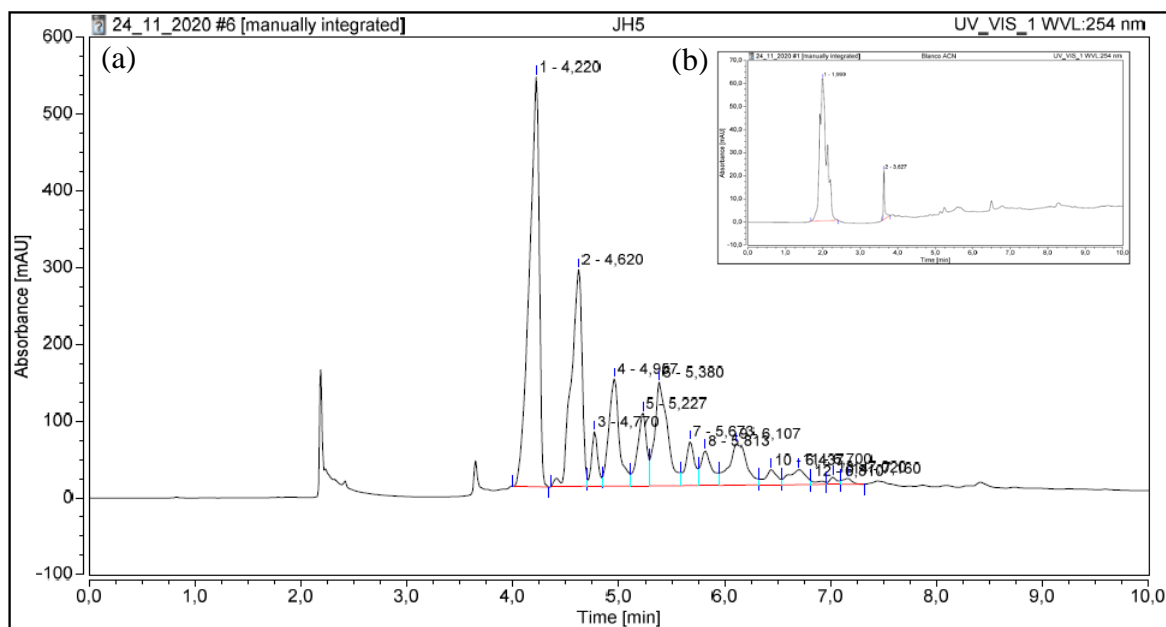


Figure 22. (a)UHPLC profile of JH5 compound, 2-(5-[6-[5-(1-carboxy-1-methylpropyl)-2-thioxo-1,3,5-thiadiazinan-3-yl]butyl]-6-thioxo-1,3,5-thiadiazin-3-yl)-3-methylbutanoic acid. (b)UHPLC profile of acetonitrile blank

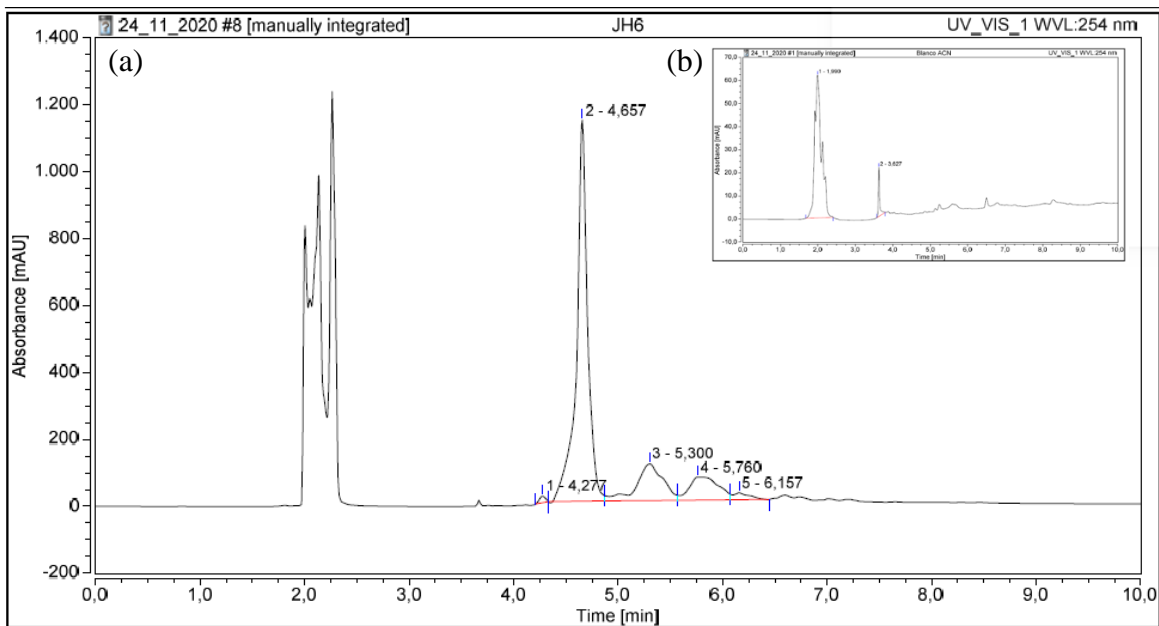


Figure 23. (a)UHPLC profile of JH6 compound, 2-(5-{6-[5-(1-carboxy-1-methylpropyl)-2-thioxo-1,3,5-thiadiazinan-3-yl] hexyl}-6-thioxo-1,3,5-thiadiazin-3-yl)-3-methylbutanoic acid. (b)UHPLC profile of acetonitrile blank

Characterization techniques (melting point, UV/Vis, and FT-IR) allowed us to confirm bis-THTT structures presence, assigning the signals to the most representatives functional groups. On the other hand, UHPLC analysis showed that JH1, JH2, JH4, and JH6 had acceptable degree purities, while JH3 and JH5 were recrystallized to achieve better purities.

6.2 Evaluation of the experimental compounds by indirect ELISA test

Hyperimmune serum was obtained from BALB/c mice inoculated with compounds derived from bis-THTT, to determine the humoral immune response by indirect ELISA test. To standardize this test, we used 1:200 dilutions of sera and 10 µg/ml concentration of the antigens. Dr. Spencer's group determinate the dilution serum and concentration in a previous study (Loachamin et al., 2019). However, the experiments of indirect ELISA were repeated three times until getting more accurate and precise results.

6.2.1 Solubility behavior of THTTs in DMSO.

It is well known that some organic compounds have solubility problems in the water, becoming a challenge when conducting biological tests. In these cases, co-solvents such as dimethylsulfoxide (DMSO), dimethylformamide (DMF), or acetonitrile (ACN), among others, should be used due to their ability to dissolve a wide range of compounds (Senac et al., 2018). In the present research, the concentration used for the six mother solutions of CQ and the bis-THTTs was 100 mg/ml. The CQ and each bis-THTT (JH1, JH2, JH3, JH4, JH5, and JH6) were diluted in a specific water volume, and the corresponding suspensions were obtained. Then, DMSO was added (10 µl each time) followed by vigorous shaking until each sample's total dissolution. The added DMSO volumes are shown in table 6.

To establish the analyzed compounds' solubility behavior, we correlate the DMSO added with the lack of solubility in water for all molecules (CQ, JH1, JH2, JH3, JH4, JH5,

and JH6) and with its structural features. Table 6 shows that CQ only needs 30 ml of DMSO to dissolve, so, as expected, it was the most soluble in water. This result is consistent with its lower mass and with the presence of secondary and tertiary amines in a flexible carbon chain.

Related to the bis-THTTs derivatives, their water solubility should be directly associated with their structures. As mentioned before, JH's are two THTT rings connected through both N3 positions by four carbons alkyl chain for JH1, JH3, JH5, and six carbons alkyl chain for JH2, JH4, and JH6. Gly substitutes the N5 positions in each compound for JH1 and JH2, Leu for JH3 and JH4, and Val for JH5 and JH6. In this context, those pair with the most simply amino acid as the substitute of N5 positions were the most soluble of the bis-THTTs. Between them, the compound JH1, which has the smallest alkyl chain as the linker of both bis-THTTs, was the most soluble in aqueous media. Similar behavior was observed for the other two pairs JH3 and JH4, and JH5 and JH6.

Table 6. Distribution of compounds diluted with DMSO

Compound	CQ	JH1	JH2	JH3	JH4	JH5	JH6
DMSO (µl)	30	80	60	140	190	200	250

6.2.2 Determination of time reaction of each experimental compound in ELISA test.

The following figures (Figures 24, 25, 26, 27, 28, 29, and 30) represent the reactions of the humoral response with the different hyperimmune sera and their antigens, where it is shown that there are differences in the reading times for detect humoral response compared to pre-immune serum.

Figure 24 shows indirect ELISA test results with an antigen concentration of 10 µg/ml (Chloroquine) and 1:200 dilutions of sera. The readings of the reaction were made every 5 minutes, from time 0 minute until 60 minutes. If we compared the time reaction of the pre-immune (PIS) and hyper-immune sera (CQS), the best time to observe the difference between PIS and CQS was at 10 minutes.

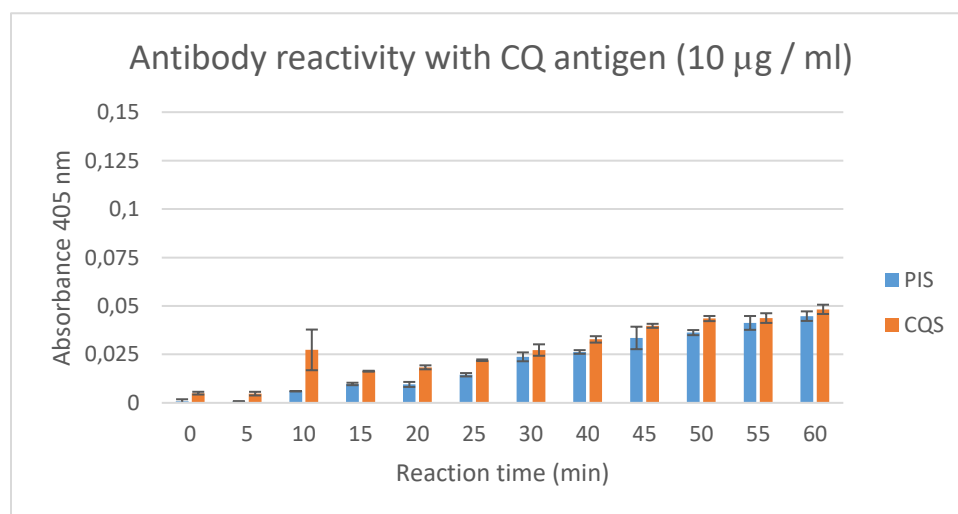


Figure 24. Indirect ELISA results, antibody (pre-immune called PIS and hyper-immune sera CQS) reactivity with antigen (CQ compound). On the X-axis are represented the time of reading of reaction vs. absorbance at 405 nm on the Y-axis, and on the bars, the standard error is represented by a black line.

Figure 25 shows indirect ELISA results with an antigen concentration of 10 µg/ml (JH1) and 1:200 dilutions of sera. The readings of the reaction were made every five minutes, from time 0 until 60 minutes. If we compared the pre-immune (PIS) and hyper-immune sera (JH1S) time reaction, the best time to observe the difference between PIS and JH1S was at 15 minutes.

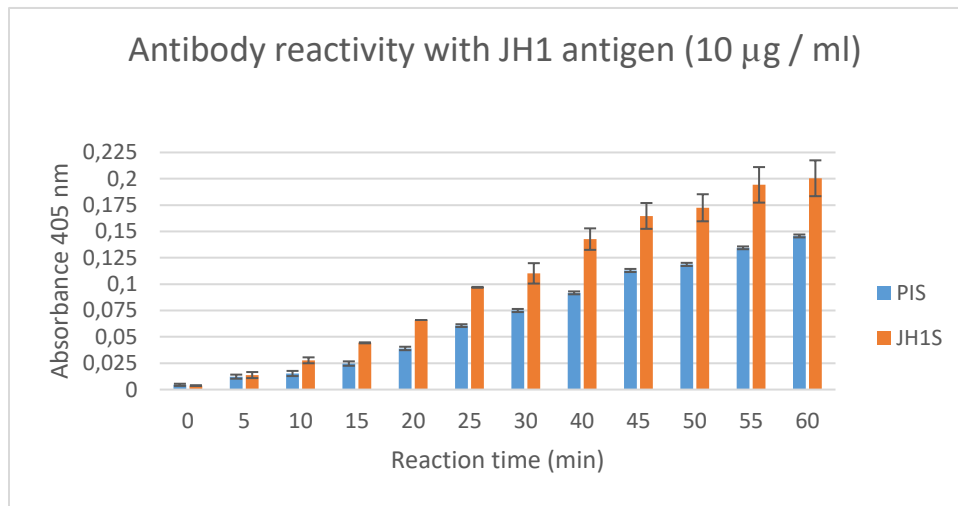


Figure 25. Indirect ELISA results, antibody (pre-immune called PIS and hyper-immune sera JH1S) reactivity with antigen (JH1 compound). On the X-axis are represented the time of reading of reaction vs. absorbance at 405 nm on the Y-axis, and on the bars, the standard error is represented by a black line.

Figure 26 shows indirect ELISA test results with an antigen concentration of 10 µg/ml (JH2) and 1:200 dilutions of sera. The readings of the reaction were made every 5 minutes, from time 0 until 60 minutes. If we compared the pre-immune (PIS) and hyper-immune sera (JH2S) time reaction, the best time to observe the difference between PIS and JH2S was at 15 minutes.

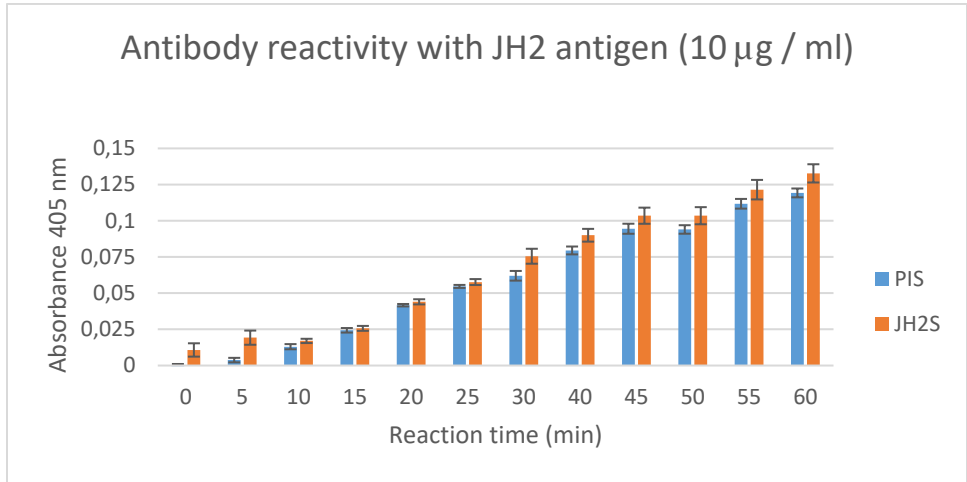


Figure 26. Indirect ELISA results, antibody (pre-immune called PIS and hyper-immune sera JH2S) reactivity with antigen (JH2 compound). On the X-axis are represented the time of reading of reaction vs. absorbance at 405 nm on the Y-axis, and on the bars, the standard error is represented by a black line.

Figure 27 shows indirect ELISA test results with an antigen concentration of 10 µg/ml (JH3) and 1:200 dilutions of sera. The readings of the reaction were made every 5 minutes, from time 0 until 60 minutes. If we compared the pre-immune (PIS) and hyper-immune sera (JH3S) time reaction, the best time to observe the difference between PIS and JH3S was at 20 minutes.

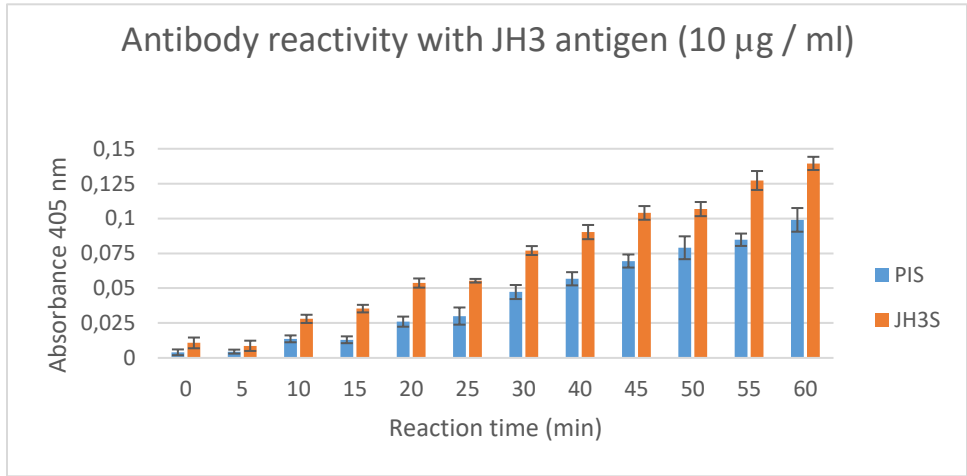


Figure 27. Indirect ELISA results, antibody (pre-immune called PIS and hyper-immune sera JH3S) reactivity with antigen (JH3 compound). On the X-axis are represented the time of reading of reaction vs. absorbance at 405 nm on the Y-axis, and on the bars, the standard error is represented by a black line.

Figure 28 shows indirect ELISA test results with an antigen concentration of 10 µg/ml (JH4) and 1:200 dilutions of sera. The readings of the reaction were made every 5 minutes, from time 0 minute until 60 minutes. If we compared the pre-immune (PIS) and hyper-

immune sera (JH4S) time reaction, the best time to observe the difference between PIS and JH4S was at 20 minutes.

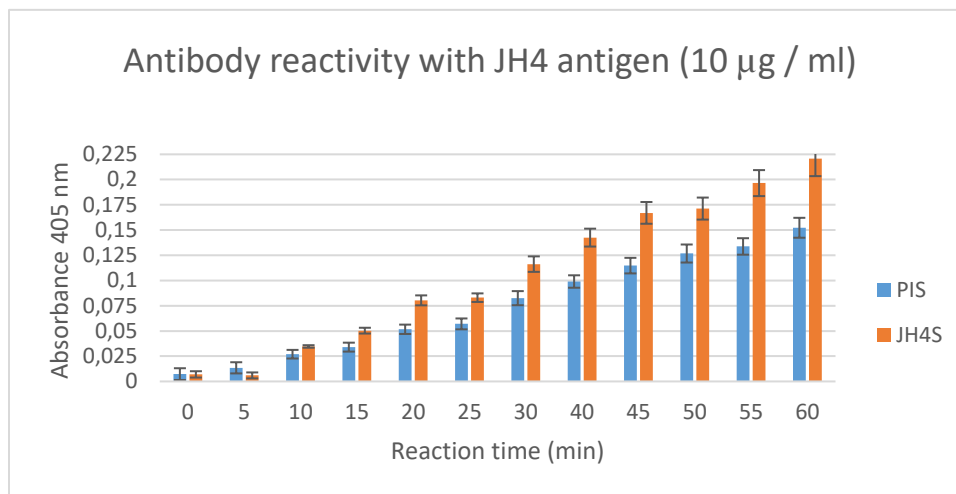


Figure 28. Indirect ELISA results, antibody (pre-immune called PIS and hyper-immune sera JH4S) reactivity with antigen (JH4 compound). On the X-axis are represented the time of reading of reaction vs. absorbance at 405 nm on the Y-axis, and on the bars, the standard error is represented by a black line.

Figure 29 shows indirect ELISA test results with an antigen concentration of 10 µg/ml (JH5) and 1:200 dilutions of sera. The readings of the reaction were made every 5 minutes, from time 0 minute until 60 minutes. If we compared the pre-immune (PIS) and hyper-immune sera (JH5S) time reaction, the best time to observe the difference between PIS and JH5S was at 20 minutes.

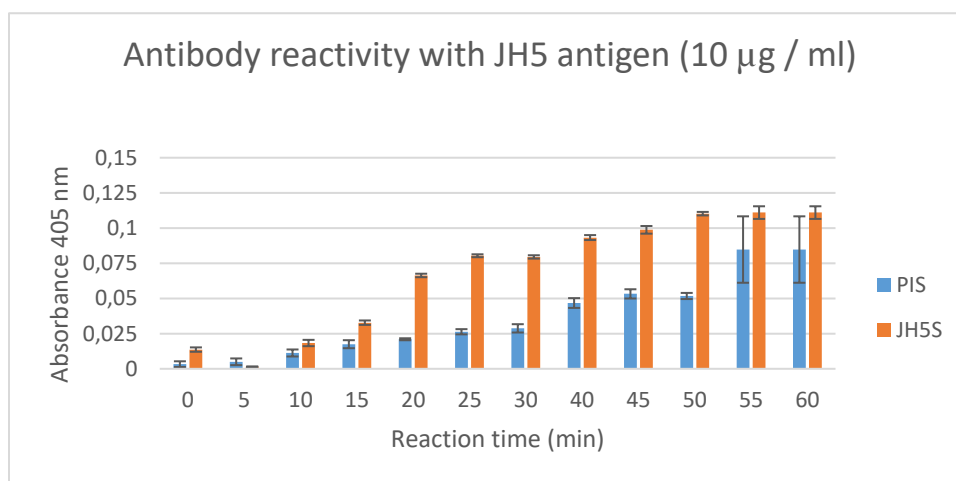


Figure 29. Indirect ELISA results, antibody (pre-immune called PIS and hyper-immune sera JH5S) reactivity with antigen (JH5 compound). On the X-axis are represented the time of reading of reaction vs. absorbance at 405 nm on the Y-axis, and on the bars, the standard error is represented by a black line.

Figure 30 shows indirect ELISA test results with an antigen concentration of 10 $\mu\text{g/ml}$ (JH6) and 1:200 dilutions of sera. The readings of the reaction were made every 5 minutes, from time 0 minute until 60 minutes. If we compared the pre-immune (PIS) and hyper-immune sera (JH6S) time reaction, the best time to observe the difference between PIS and JH6S was at 20 minutes.

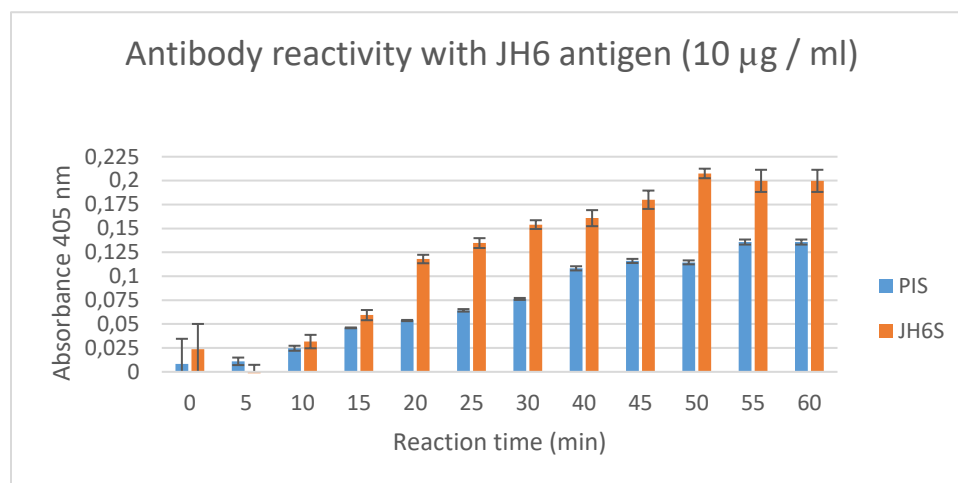


Figure 30. Indirect ELISA results, antibody (pre-immune called PIS and hyper-immune sera JH6S) reactivity with antigen (JH6 compound). On the X-axis are represented the time of reading of reaction vs. absorbance at 405 nm on the Y-axis, and on the bars, the standard error is represented by a black line.

Most of the reactions present bigger differences to compare the PIS and the hyper-immune serum at 20 minutes, except for the CQ, JH1, and JH2 antigens at 10 and 15 minutes, respectively. As can be observed, all the compounds present immunogenicity but in different degrees. Therefore, the CQ showed the lowest antibody response (0.025 O.D.), and the most immunogenic were JH4, followed by JH1 with absorbances of 0.225 and 0.200, respectively.

6.2.3 Cross-reactivity between experimental compounds

The bis-THTT have similar chemical structures. Therefore, these compounds are expected to have cross-reactivity between them. Understanding, the results may be due to the non-polar aliphatic amino acids (glycine, leucine, and valine) that each compound possesses or along the compound's chain (six carbons or four carbons). Therefore, according to the amino acids as substituents at the N-5 position, the chemical structure is JH1 and JH2 have glycine, JH3 and JH4 have leucine, JH5 JH6 have valine. . According to the chain's length, the chemical structure is that JH1, JH3, and JH5 have four carbons linked to the two N, N heterocycles, and the compounds JH2, JH4, and JH6 have six carbons joined the two N, N heterocycles.

Figure 31 presents the cross-reactivity between bis-THTT compounds with pre-immune and hyperimmune serum evaluated in the indirect ELISA test. Panel A.1 shows CQ recognition results by polyclonal antibodies in hyper-immune and pre-immune sera, this last as control of reactivity in the indirect ELISA. The absorbance values were subtracted from the PBS value as a blank.

The absorbances with the different antigens are represented in the same way. In panel A.2 for compound JH1, A.3 for compound JH2, A.4 for compound JH3, A.5 for compound JH4, A.6 for compound JH5, and A.7 for compound JH6.

The reaction reading time chosen to compare cross-reactivity was 10 minutes when the onset of absorbance differences between hyper-immune and pre-immune sera, and the value for each pre-immune serum is less than the value for each hyper-immune serum to each antigen.

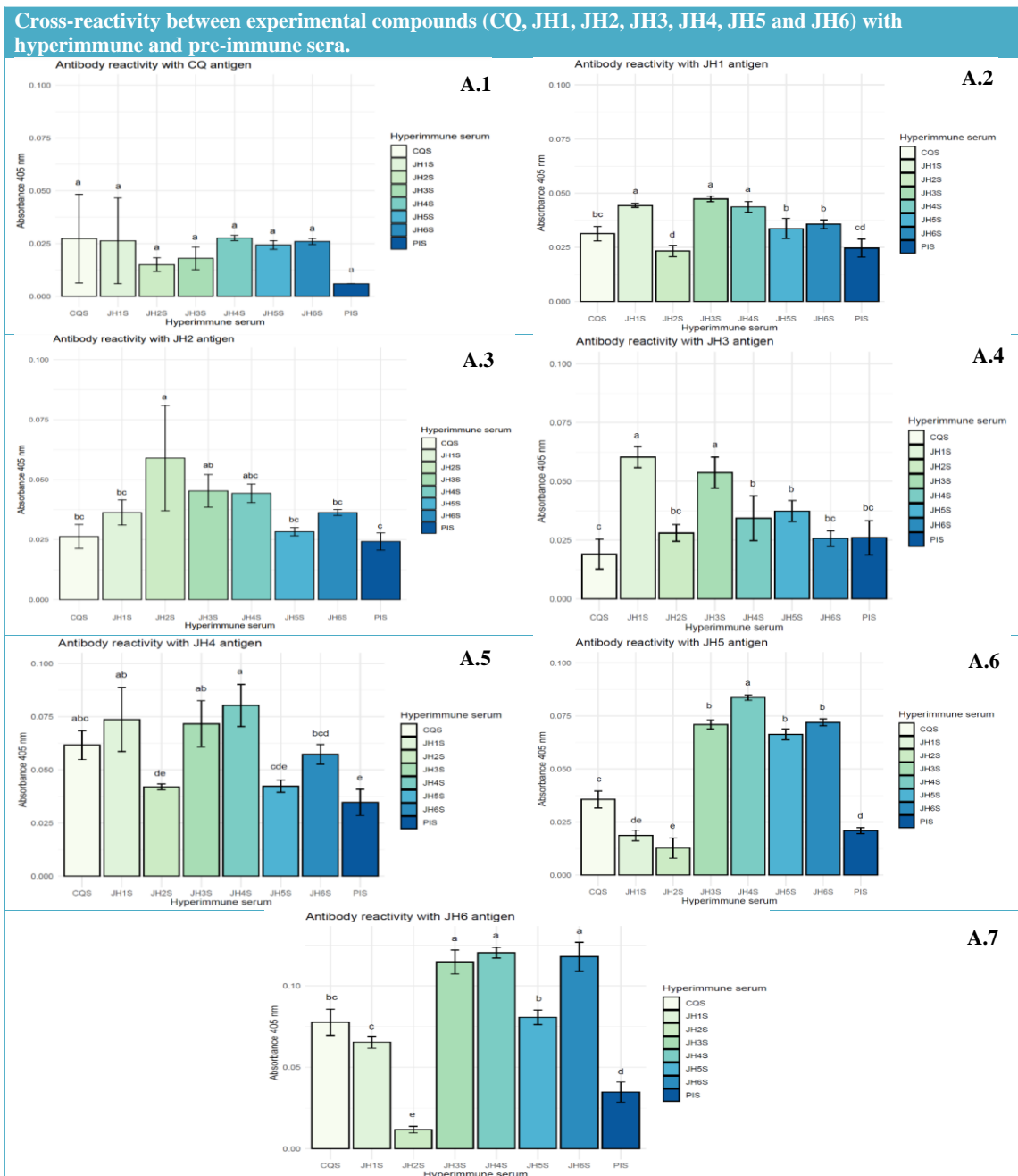


Figure 31. Results of indirect ELISA (Panels A.1, A.2, A.3, A.4, A.5, A.6, and A.7), with 10 µg/ml concentration of antigens (CQ, JH1, JH2, JH3, JH4, and JH6 compounds). On the X-axis are represented the 1:200 dilutions of the hyperimmune sera vs. absorbance at 405 nm on the Y-axis.

The different graphics show the antibodies' recognition, which represented a cross-reactivity between the six experimental compounds. A black line represents CQ with hyper-immune and pre-immune sera as bars. The standard error is shown above them. Furthermore, the letter a, b, c, d, and e represent the significant difference in the mean absorbances between the polyclonal sera due to the statistical Tukey test.

Panel A.1 shows the absorbances obtained by the hyperimmune sera and PIS for the CQ antigen. Its own hyperimmune serum CQS recognizes CQ with an absorbance of 0.027, and the second absorbance value obtained was JH4S with an absorbance of 0.028 and JH1S as the third absorbance with 0.026. The letters (a) obtained in the Turkey test represent that all sera recognize CQ as an antigen but in different magnitudes. This suggests that there is cross-reactivity between CQ, JH1, and JH4.

Panel A.2 shows the absorbances obtained by the hyperimmune sera and PIS for the JH1 antigen. In this case, its own hyperimmune serum JH1S recognizes JH1 with an absorbance of 0.04, and the second absorbance value obtained was JH3S with an absorbance of 0.047 and JH4S as the third absorbance with 0.044. The letters (a) obtained in the Turkey test represent that all sera recognize JH1 as an antigen but in different magnitudes. These results suggest that there is cross-reactivity between JH1, JH3, and JH4.

Panel A.3 shows the absorbances obtained by the hyperimmune sera and PIS for the JH2 antigen. Its own hyperimmune serum JH2S recognizes JH2 with an absorbance of 0.059, and the second absorbance value obtained was JH3S with an absorbance of 0.045 and JH4S as the third absorbance with 0.044. The letters (a) obtained in the Turkey test represent that all sera recognize JH2 as an antigen but in different magnitudes. This suggests that there is cross-reactivity very similar between JH2, JH3, and JH4.

Panel A.4 shows the absorbances obtained by the hyperimmune sera and PIS for the JH3 antigen. In this case, the first absorbance value obtained was JH1S with an absorbance of 0.060, and the second absorbance value obtained was JH3S with an absorbance of 0.054. The letters (a) obtained in the Turkey test represent that all sera recognize JH3 as an antigen but in different magnitudes. This suggests that there is cross-reactivity very similar between JH3 and JH3.

Panel A.5 shows the absorbances obtained by the hyperimmune sera and PIS for the JH4 antigen. Its own hyperimmune serum JH4S recognizes JH4 with an absorbance of 0.080, and the second absorbance value obtained was JH1S with an absorbance of 0.074 and JH3S as the third absorbance with 0.072. The letters (a) obtained in the Turkey test represent that all sera recognize JH4 as an antigen but in different magnitudes. These results suggest that there is cross-reactivity very similar between JH4, JH1, and JH3.

Panel A.6 shows the absorbances obtained by the hyperimmune sera and PIS for the JH5 antigen. In this case, the first absorbance value obtained was JH4S with an absorbance of 0.084, and the second absorbance value obtained was JH6S with an absorbance of 0.072 and JH5S as the third absorbance with 0.066. The letters (a, b) obtained in the Turkey test represent that all sera recognize JH5 as an antigen but in different magnitudes. These results suggest that there is cross-reactivity very similar between JH5, JH4, and JH6.

Panel A.7 shows the absorbances obtained by the hyperimmune sera and PIS for the JH6 antigen. Its own hyperimmune serum JH6S recognizes JH6 with an absorbance of 0.118,

and the second absorbance value obtained was JH4S with an absorbance of 0.120 and JH3S as the third absorbance with 0.114. The letters (a) obtained in the Turkey test represent that all sera recognize JH4 as an antigen but in different magnitudes. This suggests that there is cross-reactivity very similar between JH6, JH4, and JH3.

In general, JH1, JH3, and JH4 react with almost all polyclonal antibodies from different antigens. The JH6 antigen-stimulated the vertebrate BALB/c mice's immune system and presented the highest absorbance with its antigen, which was 0.118.

In summary, the cross-reactivity results outlined in Figure 31 and Table 7 suggest that the most immunogenic compounds are JH1, JH3, and JH4, presenting four to six cross-reactions. On the other hand, the least immunogenic are chloroquine, JH2, and JH5 (see table 7), and the compound that is most immunogenic for the BALB/c rodent model was JH6.

These results suggest the chemical structures that present the same substitutive amino acid is not relevant in most THTTs except the compounds JH3 and JH4 that present Leucine and vary in the carbon chain that separates them. This indicates that polyclonal antibodies recognize these two compounds and propose using combined therapies and even with JH1.

Related to the high immunogenicity of the JH6, this suggests that it is not a good quantity for the drug since it activates the vertebrate's humoral response. Furthermore, the JH3S and JH4S sera also recognize JH6 with absorbance values over 0.100, suggesting that JH6 is structurally very similar to these compounds. The difference of one more CH₂ in leucine is not relevant concerning valine in the structure recognized by antibodies.

The following table shows the summary of the results obtained in ELISA experiment of cross-reactivity between experimental compounds as antigens (CQ, JH1, JH2, JH3, JH4, JH5, and JH6), and hyperimmune sera (CQS, JH1S, JH2S, JH3S, JH4S, JH5S, and JH6S) as primary antibodies. The first row of the table shows the hyperimmune sera, and the first column of the table shows the experimental compounds. As shown in table 7, CQ is recognized by its serum and by JH1S, JH4S, JH5S, and JH6S. The compound JH1 is recognized by its serum and also by JH3S and JH4S. The compound JH2, in addition to its own recognition, is recognized by JH1S, JH3S, JH4S, and JH6S. The compound JH3 is recognized by your own serum and also by JH1S. The compound JH4 is recognized by its serum and CQS, JH1S, and JH3S sera. The compound JH5 is recognized by its serum and by JH3S, JH4S, and JH6S. Finally, the compound JH6 is recognized by its serum and by JH3S and JH4S.

Table 7. Summary of the results obtained in ELISA experiment of cross-reactivity of antibody with antigen, where + means the presence of cross-reactivity and – means there is not cross reactivity.

	CQS	JH1S	JH2S	JH3S	JH4S	JH5S	JH6S
CQ	+	+	-	-	+	+	+
JH1	-	+	-	+	+	-	-
JH2	-	+	+	+	+	-	+
JH3	-	+	-	+	-	-	-
JH4	+	+	-	+	+	-	-
JH5	-	-	-	+	+	+	+
JH6	-	-	-	+	+	-	+

Table 7 shows the match that the serum presents with its own compound, and from there the cross-reactivities with the first two compounds are deduced. Based on this, an

ELISA is made with combined antigens in the same proportion that will be explained in the next section.

6.2.4 Determination of time reaction of each combination of experimental compounds in ELISA test.

The following table shows the cross-reactivity and the order by the absorbances obtained in the previous experiments. The sera's order that recognizes their own antigen is highlighted. This table allowed us to globally view the results to choose, which would be the combinations of the compounds to be tested with the hyperimmune sera in an indirect ELISA assay.

Table 8. Cross-reactivity of antibody with antigen from highest to the lowest humoral response. In each antigen, the order of the cross-reactivity is presented, and each own hyperimmune sera is highlighted in bold.

Experimental compounds	Cross reactivity response
CQ	CQS >JH4S>JH1S>JH6
JH1	JH3S> JH1S >JH4S
JH2	JH3S>JH4S> JH2S
JH3	JH1S> JH3S >JH5S
JH4	JH4S >JH1S>JH3S>CQS
JH5	JH4S>JH6S>JH3S> JH5S
JH6	JH4S> JH6S >JH3S

For this section, the first two compounds of each cross-reactivity obtained by each experimental compound were selected. In total, 11 antigen combinations resulted. An indirect ELISA test was made using antigens: CQ+JH1, CQ+JH4, JH1+JH3, JH1+JH4, JH2+JH3, JH2+JH4, JH4+JH3, JH5+JH4, JH5+JH6, JH6+JH4, JH6+JH3, pre-immune, and antigen serum to see the cross-reactivity.

An example of the humoral response time analysis is the combination of JH1 + JH3 shown in figure 32. The results obtained in the experiment show that 20 minutes is the best time to see the difference between pre-immune and hyperimmune sera in all combinations of antigens.

Figure 32 shows the indirect ELISA results with an antigen concentration of 10 µg/ml (JH1+JH3) and 1:200 dilutions of sera. The readings of the assay were made every 5 minutes, from time 0 minute until 30 minutes. If we compared the pre-immune (PIS) reaction time and hyper-immune sera (CQS), the best time to observe the difference between PIS and JH1S and JH3S was at 20 minutes.

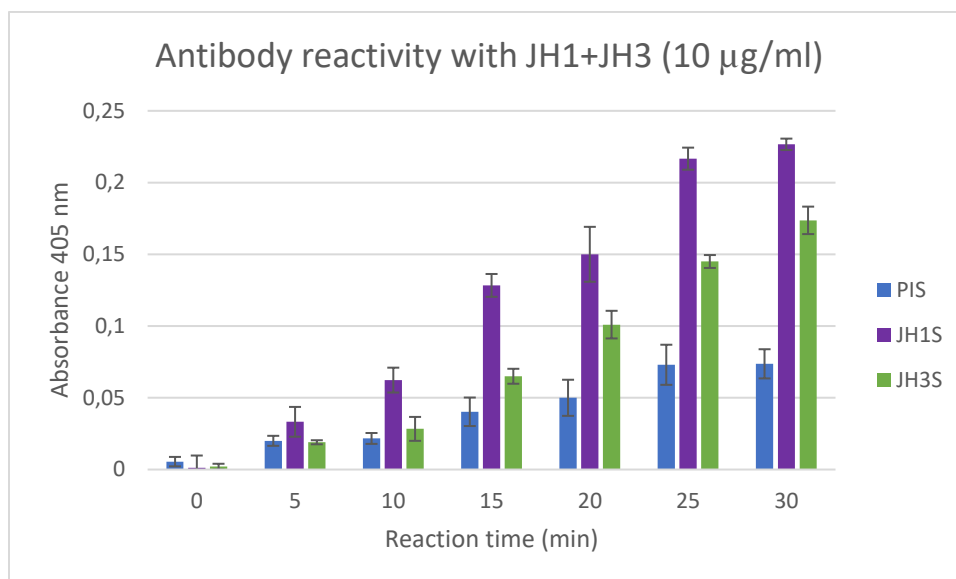


Figure 32. Indirect ELISA results, antibody (pre-immune called PIS and hyper-immune JH1S, JH3S) reactivity with antigen (JH1+JH3 compounds). On the X-axis are represented the time of reading of reaction vs. absorbance at 405 nm on the Y-axis, and on the bars the standard error is represented by a black line.

The results for the other compounds used as antigens are shown in the corresponding Annexes (Annexes 9, 10, 11, 12, 13, 14, 15, 16, 17, and 18).

6.2.5 Evaluation of cross-reactivity between the combination of two compounds as antigens in indirect ELISA

Indirect ELISA tests of figure 33 were performed with the combination of the following antigens: CQ + JH1, CQ + JH4, JH1 + JH3, JH1 + JH4, JH2 + JH3, JH2 + JH4, JH4 + JH3, JH5 + JH4, JH5 + JH6, JH6 + JH4, JH6 + JH3. Pre-immune and hyper-immune sera exposed to the combined antigens were evaluated in the immunological test. The absorbance values were subtracted from the PBS value as a blank. Each pre-immune serum's value is less than the value for each hyper-immune sera to each antigen. Finally, the absorbances between the sera were compared, and 20 minutes was chosen as the reading time to compare the ELISA results with the combined antigens.

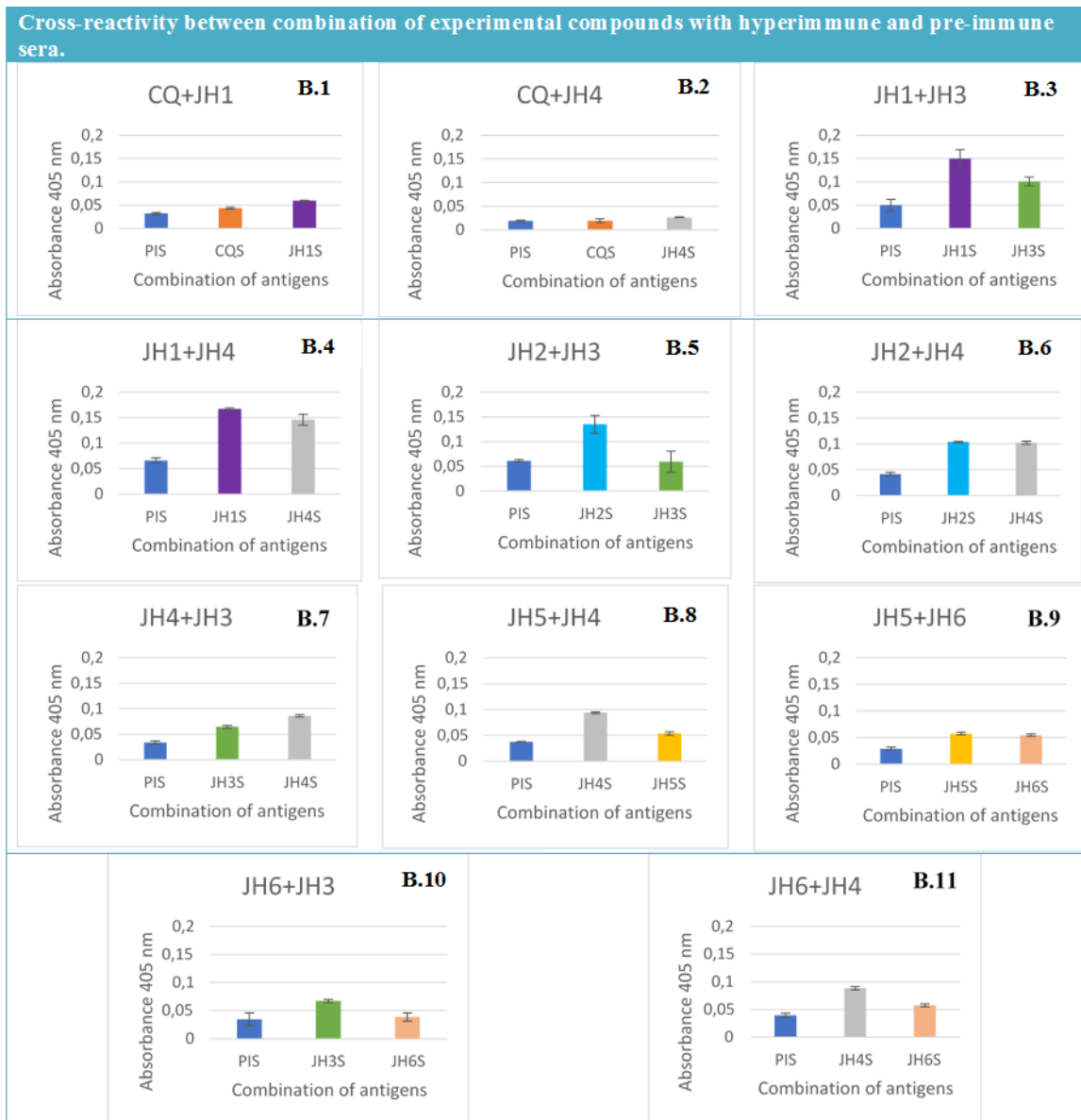


Figure 33. Results of indirect ELISA (Panels B.1, B.2, B.3, B.4, B.5, B.6, B.7, B.8, B.9, B.10 and B.11) at 20 minutes, with 10 $\mu\text{g/ml}$ concentration of combination of antigens (CQ+JH1, CQ+JH4, JH1+JH3, JH1+JH4, JH2+JH3, JH2+JH4, JH4+JH3, JH5+JH4, JH5+JH6, JH6+JH4, JH6+JH3). On the X-axis is represented the combination of antigens vs. absorbance at 405 nm on the Y-axis. The graphic shows the antibodies' recognition, which represented a cross-reactivity between the combination of antigens with hyper-immune and pre-immune sera as bars. A black line above them represents the standard error.

The analysis for figure 33 follows the following order:

Panel B.1 shows the absorbances obtained by the hyperimmune sera and PIS for the combination of antigens CQ + JH1. The highest recognition was JH1S, indirectly representing a higher concentration of antibodies with an absorbance of 0.059. CQS is very poorly immunogenic, as we saw in panel A.1 of figure 31 and has an absorbance of 0.043.

Panel B.2 shows the absorbances obtained by the hyperimmune sera and PIS for the combination of antigens CQ + JH4. This combination shows no significant difference between the hyperimmune sera because they have similar absorbances. CQS has an absorbance of 0.019, and JH4S has an absorbance of 0.026. So, there is no domain with antigenicity; that is, the two compounds are not antigenic.

Panel B.3 shows the absorbances obtained by the hyperimmune sera and PIS for the combination of antigens JH1 + JH3: JH1S is the most immunogenic, and there is a higher concentration of antibodies because it has the highest absorbance in the combination. The absorbance of JH1S is 0.15, while the absorbance of JH3S is 0.101.

Panel B.4 shows the absorbances obtained by the hyperimmune sera and PIS for the combination of antigens JH1 + JH4. JH1S presented 0.167 absorbances, and JH4S 0.146 absorbance. Therefore, it can be mentioned that there is mutual recognition by antigens because the absorbance amounts are similar.

Panel B.5 shows the absorbances obtained by the hyperimmune sera and PIS for the combination of antigens JH2 + JH3. JH2S is the most immunogenic, and there is a higher recognition of antibodies because it presents the highest absorbance in the combination. The absorbance of JH2S is 0.135, while the absorbance of JH3S is 0.059.

Panel B.6 shows the absorbances obtained by the hyperimmune sera and PIS for the combination of antigens JH2 + JH4. This combination shows double recognition because the absorbances of the sera are similar. JH2S has an absorbance of 0.104, and JH4S has 0.102 absorbances.

Panel B.7 shows the absorbances obtained by the hyperimmune sera and PIS for the combination of antigens JH4 + JH3. The highest recognition was JH4S, indirectly representing a higher concentration of antibodies with an absorbance of 0.086. JH3S is less immunogenic and has an absorbance of 0.064.

Panel B.8 shows the absorbances obtained by the hyperimmune sera and PIS for the combination of antigens JH5 + JH4. JH4S is the most immunogenic, and there is a higher concentration of antibodies because it has the highest absorbance in the combination. The absorbance of JH4S is 0.093, while the absorbance of JH5S is 0.053.

Panel B.9 shows the absorbances obtained by the hyperimmune sera and PIS for the combination of antigens JH5 + JH6. This combination shows double recognition because the absorbances of the sera are similar. JH5S presents an absorbance of 0.057, and JH6S an absorbance of 0.054.

Panel B.10 shows the absorbances obtained by the hyperimmune sera and PIS for the combination of antigens JH6 + JH4. JH4S is the most immunogenic, and there is a higher recognition of antibodies because it presents the highest absorbance in the combination. The absorbance of JH4S is 0.088, while the absorbance of JH6S is 0.057.

Panel B.11 shows the absorbances obtained by the hyperimmune sera and PIS for the combination of antigens JH6 + JH3. JH3S presents an absorbance of 0.067, while JH6S an absorbance of 0.038. Its own antibodies most recognize JH3S than JH6.

Finally, we suggest that the best combinations of two antigens as a combined therapy would be: JH1 + JH3, JH1 + JH4, JH2 + JH3, and JH2 + JH4. Because they share similar absorbances between the mixture of antigens, suggesting a similar recognition by the antibodies of both hyperimmune sera between both compounds combined, which could be used in combination therapy in a murine malaria model.

There are references to experiments with cross-reactivity between antigens, as shown in section 2.9 of the introduction. Therefore, it is the first time that a cross-reactivity

experiment has been carried out with antibodies (hyperimmune sera) obtained from BALB/c mice and that there is recognition with antigens that are the experimental compounds with certain antimalarial activity derived from thiadiazine.

7. CONCLUSION

The six bis-THTT (JH1-JH6) were characterized using melting point (mp), FT-IR, and UV/Vis spectroscopy to verify the compound's structure. UHPLC results demonstrate an acceptable degree of purity for JH1, JH2, JH4, and JH6, while JH3 and JH5 were recrystallized to be used as antigens in the generation of hyperimmune sera obtained from immunized BALB / c mice.

The experimental compounds of this study have similar structures. Therefore, the cross-reactivity evaluation was a good strategy to determine the analysis by antibody recognition. The humoral evaluation results through the indirect ELISA show that compounds JH1, JH3, and JH4 react with almost all of them or are recognized by the rest of the compounds' polyclonal antibodies. The JH4, JH5, and JH6 antigens stimulated the BALB/C mice immune presented the highest absorbances. Therefore, compound JH6 showed the highest antibody response (0.118 O.D.) followed by JH4 and JH5 with absorbances of 0.080 and 0.066, respectively. In contrast, the antigens with less humoral response stimulation are CQ with an absorbance of 0.027, followed by JH1 with an absorbance of 0.044. Therefore, they are the least immunogenic because they do not present a greater humoral response.

Finally, in the cross-reactivity experiment, it is obtained that the combinations JH1 + JH3, JH1 + JH4, JH2 + JH3, and JH2 JH4 could be used as combination therapy because they share absorbances between the mixture of antigens. These suggest a recognition by antibodies show the similar structure as epitopes into the Fab region of antibodies by compounds.

8. REFERENCES

- Abdulkadir, A. (2019). The Benefits of Chloroquine Multi-Mechanisms of Action on the Nervous System. *Theranostics Brain,Spine & Neural Disord.* <https://doi.org/10.19080/JOJS.2019.03.555606>
- Aguiar, A. C. C., Murce, E., Cortopassi, W. A., Pimentel, A. S., Almeida, M. M. F. S., Barros, D. C. S., Guedes, J. S., Meneghetti, M. R., & Krettli, A. U. (2018). Chloroquine analogs as antimalarial candidates with potent in vitro and in vivo activity. *International Journal for Parasitology: Drugs and Drug Resistance*, 8(3), 459–464. <https://doi.org/10.1016/j.ijpddr.2018.10.002>
- Aljamali, N. M., & Alfatlawi, I. O. (2015). Synthesis of sulfur heterocyclic compounds and study of expected biological activity. *Research Journal of Pharmacy and Technology*, 8(9), 1225–1242. <https://doi.org/10.5958/0974-360X.2015.00224.3>
- Amit Koparde, A., Chandrashekar Doijad, R., & Shripal Magdum, C. (2019). Natural Products in Drug Discovery. In *Pharmacognosy - Medicinal Plants*. IntechOpen. <https://doi.org/10.5772/intechopen.82860>
- Aydin, S. (2015). A short history, principles, and types of ELISA, and our laboratory experience with peptide/protein analyses using ELISA. *Peptides*, 72, 4–15. <https://doi.org/10.1016/j.peptides.2015.04.012>
- Barmade, M. A., & Ghuge, R. B. (2018). Vicinal Diaryl Heterocyclic System: A Privileged Scaffold in the Discovery of Potential Therapeutic Agents. In *Vicinal Diaryl Substituted Heterocycles*. Elsevier Ltd. <https://doi.org/10.1016/b978-0-08-102237-5.00001-8>
- Beck, T. (2006). Will malaria soon be a thing of the past?. *Coffee Break - NCBI Bookshelf*. <https://www.ncbi.nlm.nih.gov/books/NBK5951/>
- Bermello, J. C., Piñeiro, R. P., Fidalgo, L. M., Cabrera, H. R., & Navarro, M. S. (2011). Thiadiazine Derivatives as Antiprotozoal New Drugs. *The Open Medicinal Chemistry Journal*, 5, 51–60. <https://doi.org/10.2174/1874104501105010051>
- Bhattacharjee, S., Coppens, I., Mbengue, A., Suresh, N., Ghorbal, M., Slouka, Z., Safeukui, I., Tang, H. Y., Speicher, D. W., Stahelin, R. V., Mohandas, N., & Haldar, K. (2018). Remodeling of the malaria parasite and host human red cell by vesicle amplification that induces artemisinin resistance. *Blood*, 131(11), 1234–1247. <https://doi.org/10.1182/blood-2017-11-814665>
- Chassaigne, J. (2001). Malaria y fármacos antimaláricos. *Revista de la Sociedad Venezolana de Microbiología*. http://ve.scielo.org/scielo.php?script=sci_arttext&pid=S1315-25562001000200017
- Conrad, M. D., Nsoya, S. L., & Rosenthal, P. J. (2019). The Diversity of the Plasmodium falciparum K13 Propeller Domain Did Not Increase after Implementation of Artemisinin-Based Combination Therapy in Uganda. *Antimicrobial Agents and Chemotherapy*, 63(10), 1–8. <https://doi.org/10.1128/AAC.01234-19>
- Conrad, M. D., & Rosenthal, P. J. (2019). Antimalarial drug resistance in Africa: the calm before the storm?. *The Lancet Infectious Diseases*, 19(10), e338–e351. [https://doi.org/10.1016/S1473-3099\(19\)30261-0](https://doi.org/10.1016/S1473-3099(19)30261-0)
- Coro, J., Atherton, R., Little, S., Wharton, H., Yardley, V., Alvarez, A., Suárez, M., Pérez, R., & Rodríguez, H. (2006). Alkyl-linked bis-THTT derivatives as potent in vitro trypanocidal agents. *Bioorganic and Medicinal Chemistry Letters*, 16(5), 1312–1315. <https://doi.org/10.1016/j.bmcl.2005.11.060>
- Coro, J., Little, S., Yardley, V., Suárez, M., Rodríguez, H., Martín, N., & Perez-Pineiro, R.

- (2008). Synthesis and antiprotozoal evaluation of new N4-(benzyl) spermidyl-linked bis(1,3,5-thiadiazinane-2-thiones). *Archiv Der Pharmazie*, 341(11), 708–713. <https://doi.org/10.1002/ardp.200800011>
- Coro, J., Pérez, R., Rodríguez, H., Suárez, M., Vega, C., Rolón, M., Montero, D., Nogal, J. J., & Gómez-Barrio, A. (2005). Synthesis and antiprotozoan evaluation of new alkyl-linked bis(2-thioxo-[1,3,5]thiadiazinan-3-yl) carboxylic acids. *Bioorganic and Medicinal Chemistry*, 13(10), 3413–3421. <https://doi.org/10.1016/j.bmc.2005.03.009>
- Cui, L., & Su, X. Z. (2009). Discovery, mechanisms of action and combination therapy of artemisinin. *Expert Review of Anti-Infective Therapy*, 7(8), 999–1013. <https://doi.org/10.1586/ERI.09.68>
- Diarra, A., Nebie, I., Tiono, A., Soulama, I., Ouedraogo, A., Konate, A., Theisen, M., Doodoo, D., Traore, A., & Sirima, S. B. (2012). Antibodies to malaria vaccine candidates are associated with chloroquine or sulphadoxine/pyrimethamine treatment efficacy in children in an endemic area of Burkina Faso. *Malaria Journal*, 11, 2–7. <https://doi.org/10.1186/1475-2875-11-79>
- Durand, R., Prendki, V., Cailhol, J., Hubert, V., Ralaimazava, P., Massias, L., Bouchaud, O., & Le Bras, J. (2008). Plasmodium falciparum malaria and atovaquone-proguanil treatment failure. *Emerging Infectious Diseases*, 14(2), 320–322. <https://doi.org/10.3201/eid1402.070945>
- Durand, S., Lachira-Alban, A., & Cabezas, C. (2018). Impact of different treatment schemes on malaria in the peruvian coast and amazon region within the framework of a policy on antimalarial medications, 1994-2017. *Revista Peruana de Medicina Experimental y Salud Publica*, 35(3), 497–504. <https://doi.org/10.17843/rpmesp.2018.353.3891>
- Fairhurst, R. M., & Dondorp, A. M. (2016). Artemisinin-Resistant Plasmodium falciparum Malaria. *National Library of Medicine*, May 2017, 1–16. <https://doi.org/10.1128/microbiolspec.EI10-0013-2016>.
- Gendrot, M., Diawara, S., Madamet, M., Kounta, M. B., Briolant, S., Wade, K. A., Fall, M., Benoit, N., Nakoulima, A., Amalvict, R., Diémé, Y., Fall, B., Wade, B., Diatta, B., & Pradines, B. (2017). Association between polymorphisms in the Pfmdr6 gene and ex vivo susceptibility to quinine in Plasmodium falciparum parasites from Dakar, Senegal. *Antimicrobial Agents and Chemotherapy*, 61(3). <https://doi.org/10.1128/AAC.01183-16>
- Giraldo, C., & Blair, S. (2003). *MEFLOQUINE*. Mefloquina. *Iatreia*, 16(1), 19-31. Retrieved February 15, 2021, from http://www.scielo.org.co/scielo.php?script=sci_arttext&pid=S0121-07932003000100003&lng=en&tlng=es.
- Gopalakrishnan, A. M., & Kumar, N. (2015). Antimalarial action of artesunate involves DNA damage mediated by reactive oxygen species. *Antimicrobial Agents and Chemotherapy*, 59(1), 317–325. <https://doi.org/10.1128/AAC.03663-14>
- IUPAC. (2014). *IUPAC Gold Book - heterocyclic compounds*. 1307, 2798. <https://doi.org/10.1351/goldbook.H02798>
- Kalaria, P. N., Karad, S. C., & Raval, D. K. (2018). A review on diverse heterocyclic compounds as the privileged scaffolds in antimalarial drug discovery. *European Journal of Medicinal Chemistry*, 158, 917–936. <https://doi.org/10.1016/j.ejmech.2018.08.040>
- Khalil, I. F., Alifrangis, M., Recke, C., Hoegberg, L. C., Bygbjerg, I. C., & Koch, C. (2011). Development of ELISA-based methods to measure the anti-malarial drug chloroquine in plasma and in pharmaceutical formulations. *Malaria Journal*, 10, 1–7.

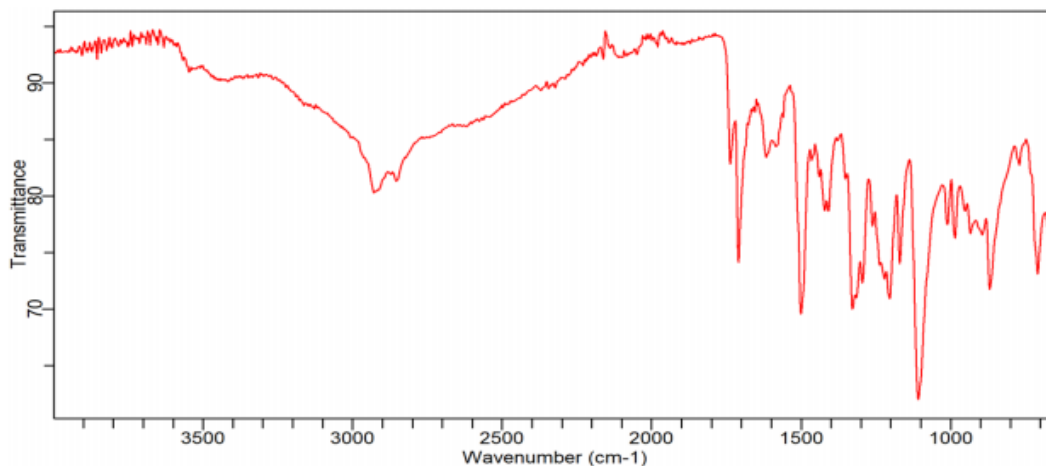
- <https://doi.org/10.1186/1475-2875-10-249>
- Kindt, T., Goldsby, R., & Osborne, B. (2007). *Kuby immunology* (6th ed.). McGraw-Hill.
- Knell, J. (1991). *Malaria : a publication of the tropical programme of the Wellcome trust - Ghent University Library*.
- Laloo, D. G. (2013). Malaria in the Returned Traveler. In *Hunter's Tropical Medicine and Emerging Infectious Disease: Ninth Edition* (pp. 1032–1036). Elsevier Inc. <https://doi.org/10.1016/B978-1-4160-4390-4.00144-2>
- Lawrenson, A. S., Cooper, D. L., O'Neill, P. M., & Berry, N. G. (2018). Study of the antimalarial activity of 4-aminoquinoline compounds against chloroquine-sensitive and chloroquine-resistant parasite strains. *Journal of Molecular Modeling*, 24(9). <https://doi.org/10.1007/s00894-018-3755-z>
- Loachamin, K. S., Rodríguez, H. M., & Spencer L.M. (2019). Effect of six bis-THTT derivatives in the control of parasitaemia in two rodent malaria species. *Bionatura*, 02(Bionatura Conference Serie), 7–12. <https://doi.org/10.21931/rb/cs/2019.02.01.11>
- Martins, P., Jesus, J., Santos, S., Raposo, L. R., Roma-Rodrigues, C., Baptista, P. V., & Fernandes, A. R. (2015). Heterocyclic anticancer compounds: Recent advances and the paradigm shift towards the use of nanomedicine's tool Box. *Molecules*, 20(9), 16852–16891. <https://doi.org/10.3390/molecules200916852>
- Meshnick, S. R. (2002). Artemisinin: Mechanisms of action, resistance and toxicity. *International Journal for Parasitology*, 32(13), 1655–1660. [https://doi.org/10.1016/S0020-7519\(02\)00194-7](https://doi.org/10.1016/S0020-7519(02)00194-7)
- Milligan, R., Daher, A., & Graves, P. M. (2019). Primaquine at alternative dosing schedules for preventing relapse in people with plasmodium vivax malaria. *Cochrane Database of Systematic Reviews*, 2019(7). <https://doi.org/10.1002/14651858.CD012656.pub2>
- Ministerio de sanidad, política, social e igualdad. (2016). Ficha técnica. *Agencia Española de Medicamentos y Productos Sanitarios (AEMPS)*
- Mitsui, Y. (2016). Development of a simple and specific direct competitive ELISA for the determination of artesunate using an anti-artesunate polyclonal antiserum. *Tropical Medicine and Health*, 4–10. <https://doi.org/10.1186/s41182-016-0037-2>
- Msellem, M., Morris, U., Soe, A., Abbas, F. B., Ali, A. W., Barnes, R., Frumento, P., Ali, A. S., Mårtensson, A., & Björkman, A. (2020). Increased Sensitivity of Plasmodium falciparum to Artesunate/Amodiaquine Despite 14 Years as First-Line Malaria Treatment, Zanzibar. *Emerging Infectious Diseases*, 26(8), 1767–1777. <https://doi.org/10.3201/eid2608.191547>
- National Center for Biotechnology Information. (2021a). (-)-Quinine | C₂₀H₂₄O₂N₂ - PubChem. <https://pubchem.ncbi.nlm.nih.gov/compound/Quinine>
- National Center for Biotechnology Information. (2021b). Artemisinin | C₁₅H₂₂O₅ - PubChem. <https://pubchem.ncbi.nlm.nih.gov/compound/Artemisinin>
- National Center for Biotechnology Information. (2021c). Chloroquine | C₁₈H₂₆ClN₃ - PubChem. <https://pubchem.ncbi.nlm.nih.gov/compound/Chloroquine>
- Nichols, L. (2020, August 14). 6.1B: Uses of Melting Points - Chemistry LibreTexts. [https://chem.libretexts.org/Bookshelves/Organic_Chemistry/Book%3A_Organic_Chemistry_Lab_Techniques_\(Nichols\)/06%3A_Miscellaneous_Techniques/6.01%3A_Melting_Point/6.1B%3A_Uses_of_Melting_Points](https://chem.libretexts.org/Bookshelves/Organic_Chemistry/Book%3A_Organic_Chemistry_Lab_Techniques_(Nichols)/06%3A_Miscellaneous_Techniques/6.01%3A_Melting_Point/6.1B%3A_Uses_of_Melting_Points)
- Ning, X., Tan, G., Chen, X., Wang, M., Wang, B., & Cui, L. (2019). Development of a lateral flow dipstick for simultaneous and semi-quantitative analysis of dihydroartemisinin and piperazine in an artemisinin combination therapy. *Drug Testing and Analysis*, 11(9),

- 1444–1452. <https://doi.org/10.1002/dta.2656>
- Noronha, M., Pawar, V., Prajapati, A., & Subramanian, R. B. (2020). A literature review on traditional herbal medicines for malaria. *South African Journal of Botany*, *128*, 292–303. <https://doi.org/10.1016/j.sajb.2019.11.017>
- Obonyo, C. O., & Juma, E. A. (2012). Clindamycin plus quinine for treating uncomplicated falciparum malaria: A systematic review and meta-analysis. *Malaria Journal* (Vol. 11, Issue 1, p. 2). BioMed Central. <https://doi.org/10.1186/1475-2875-11-2>
- Ochoa, C., Pérez, E., Pérez, R., Suárez, M., Ochoa, E., Rodríguez, H., Gómez Barrio, A., Muclas, S., José Nogal, J., & Martínez, R. A. (1999). Synthesis and antiprotozoan properties of new 3,5-disubstituted-tetrahydro-2H-1,3,5-thiadiazine-2-thione derivatives. *Arzneimittel-Forschung/Drug Research*, *49*(9), 764–769. <https://doi.org/10.1055/s-0031-1300499>
- Perez, C., & Morales, M. (2016). Lincosamidas. *Universidad de Cuenca*. <https://es.slideshare.net/MateoMoralesGonzalez2/lincosamidas-farmacologia>
- Phillips, M. A., Burrows, J. N., Manyando, C., Van Huijsduijnen, R. H., Van Voorhis, W. C., & Wells, T. N. C. (2017). Malaria. *Nature Reviews Disease Primers*, *3*. <https://doi.org/10.1038/nrdp.2017.50>
- Pinder, M., Sutherland, C. J., Sisay-Joof, F., Ismaili, J., McCall, M. B. B., Ord, R., Hallett, R., Holder, A. A., & Milligan, P. (2006). Immunoglobulin G antibodies to merozoite surface antigens are associated with recovery from chloroquine-resistant *Plasmodium falciparum* in Gambian children. *Infection and Immunity*, *74*(5), 2887–2893. <https://doi.org/10.1128/IAI.74.5.2887-2893.2006>
- Pinheiro, L. C. S., Feitosa, L. M., da Silveira, F. F., & Boechat, N. (2018). Current antimalarial therapies and advances in the development of semi-synthetic artemisinin derivatives. *Anais Da Academia Brasileira de Ciencias*, *90*(1), 1251–1271. <https://doi.org/10.1590/0001-3765201820170830>
- Pretsch, E., Bühlmann, P., & Affolter, C. (2000). Structure Determination of Organic Compounds. In *Structure Determination of Organic Compounds*. <https://doi.org/10.1007/978-3-662-04201-4>
- Rios, A., Blair, S., & Pabon, A. (2017). Avances en la búsqueda y desarrollo de quimioprofilácticos causales para malaria. *Universidad de Antioquia*. <https://www.redalyc.org/jatsRepo/1805/180550477006/html/index.html>
- Rios, C. (2019). Uso de la metabolómica para la discriminación preliminar de las variedades “chilliwa” y “ramis” de las semillas de kañiwa. *Universidad Peruana Cayetano Heredia*. http://repositorio.upch.edu.pe/bitstream/handle/upch/7674/Uso_RiosLovon_Carlos.pdf?sequence=1&isAllowed=y
- Rodríguez, C., & Obrador, G. (2013). *Antimaláricos, leishmanicidas y tripanosomicidas / Fichero farmacológico | AccessMedicina | McGraw-Hill Medical*. <https://accessmedicina.mhmedical.com/content.aspx?bookid=1510§ionid=98012128>
- Rodríguez, H., Suárez, M., & Albericio, F. (2012). Thiadiazines, N,N-heterocycles of biological relevance. *Molecules*, *17*(7), 7612–7628. <https://doi.org/10.3390/molecules17077612>
- Rodríguez, M. (2017). Synthesis and biological evaluation of sulfanyl and sulfonyl chalcones, and metronidazole derivatives with possible antimalarial and leishmanicidal activity. *Université de Bordeaux*, 56-71.
- Sabir, S., Alhazza, M. I., & Ibrahim, A. A. (2016). A review on heterocyclic moieties and

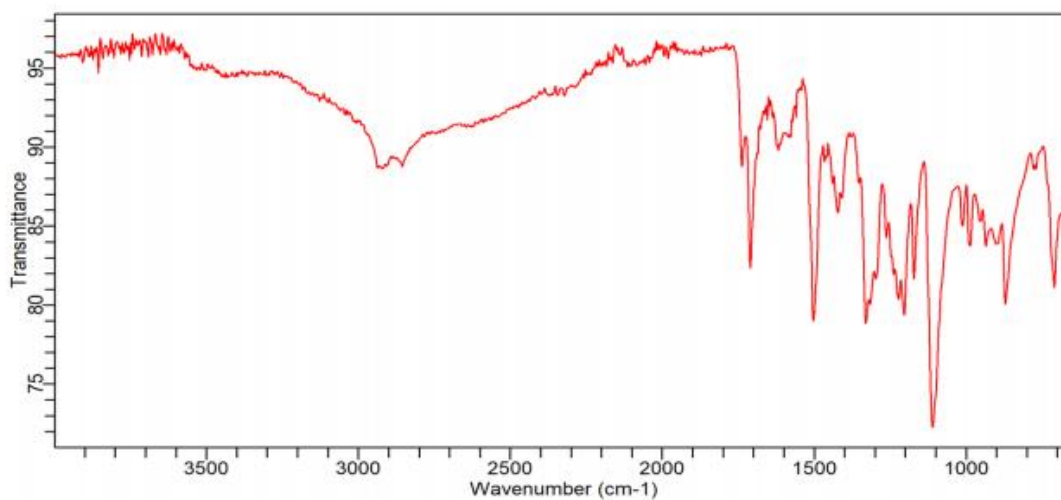
- their applications. *Catalysis for Sustainable Energy*, 2(1), 99–115. <https://doi.org/10.1515/cse-2015-0009>
- Schrezenmeier, E., & Dörner, T. (2020). Mechanisms of action of hydroxychloroquine and chloroquine: implications for rheumatology. *Nature Reviews Rheumatology*, 16(3), 155–166. <https://doi.org/10.1038/s41584-020-0372-x>
- Senac, C., Desgranges, S., Contino-Pepin, C., Urbach, W., Fuchs, P. F. J., & Taulier, N. (2018). Effect of dimethyl sulfoxide on the binding of 1-adamantane carboxylic acid to β - and γ -cyclodextrins. *ACS Omega*, 3(1), 1014–1021. <https://doi.org/10.1021/acsomega.7b01212>
- Shoemaker, A. (2002). Tratado de medicina crítica y terapia intensiva. *Google Libros*. https://books.google.com.ec/books?id=d4NfFCXqc2IC&pg=PA761&lpg=PA761&dq=quinina,quinolina&source=bl&ots=PhJPy3OgCP&sig=ACfU3U2UQ1gtNU13p7qdsu2wqjz3VS6Gsg&hl=es&sa=X&ved=2ahUKewin_rah5cjrAhXsqFkKHfAKCjQQ6AEwDHoECAEQAQ#v=onepage&q=quinina%2Cquinolina&f=false
- Sinha, S., Medhi, B., & Sehgal, R. (2014). Challenges of drug-resistant malaria. *Parasite*, 21, 61. <https://doi.org/10.1051/parasite/2014059>
- Spencer, L. M., Mendoza, E., & Louro, A. (2016). Mecanismos de invasión del esporozoíto de *Plasmodium* en el mosquito vector *Anopheles*. *Revista Bionatura*, 1(3), 146–153
- Su-ping, H., Gui-yu, T., Gang, L., & Wei-ming, T. (2009). Development of a sensitive monoclonal antibody-based enzyme-linked immunosorbent assay for the antimalaria active ingredient artemisinin in the Chinese herb *Artemisia annua* L. *Analytical and Bioanalytical Chemistry*, 393(4), 1297–1303. <https://doi.org/10.1007/s00216-008-2527-5>
- World Health Organization. (2019). World malaria report 2019. <https://apps.who.int/iris/handle/10665/330011>. License: CC BY-NC-SA 3.0 IGO.
- World Health Organization. (2015). Treatment of *Plasmodium vivax*, *P. ovale*, *P. malariae* and *P. knowlesi* infections. <https://www.ncbi.nlm.nih.gov/books/NBK294430/>
- World Health Organization. (2020). World Malaria Report. https://www.who.int/docs/default-source/malaria/world-malaria-reports/world-malaria-report-2020-briefing-kit-sp.pdf?sfvrsn=a6de03a5_11
- World Health Organization. (2015). Guidelines for the Treatment of Malaria. 3rd edition. Geneva: World Health Organization; 2015. Annex 4, Grading of Recommendations Assessment, Development and Evaluation (GRADE) for assessing the quality of evidence. *Guidelines for the Treatment of Malaria. 3rd edition*. World Health Organization. <https://www.ncbi.nlm.nih.gov/books/NBK294440/>
- World Health Organization. (2018). Malaria treatment: an overview. <https://www.who.int/malaria/areas/treatment/overview/es/>
- Yalkowsky, S. H., & Alantary, D. (2004). Estimation of Melting Points of Organics. *Industrial & Engineering Chemistry Research*, 43(23), 7618–7621. <https://doi.org/10.1016/j.xphs.2017.12.013>
- Yeo, S. J., Liu, D. X., Kim, H. S., & Park, H. (2017). Anti-malarial effect of novel chloroquine derivatives as agents for the treatment of malaria. *Malaria Journal*, 16(1), 1–9. <https://doi.org/10.1186/s12936-017-1725-z>
- York, A. (2020). The ART of solving the mystery. *Nature Reviews Microbiology*, 18(3), 121. <https://doi.org/10.1038/s41579-020-0326-y>

9. ANNEXES

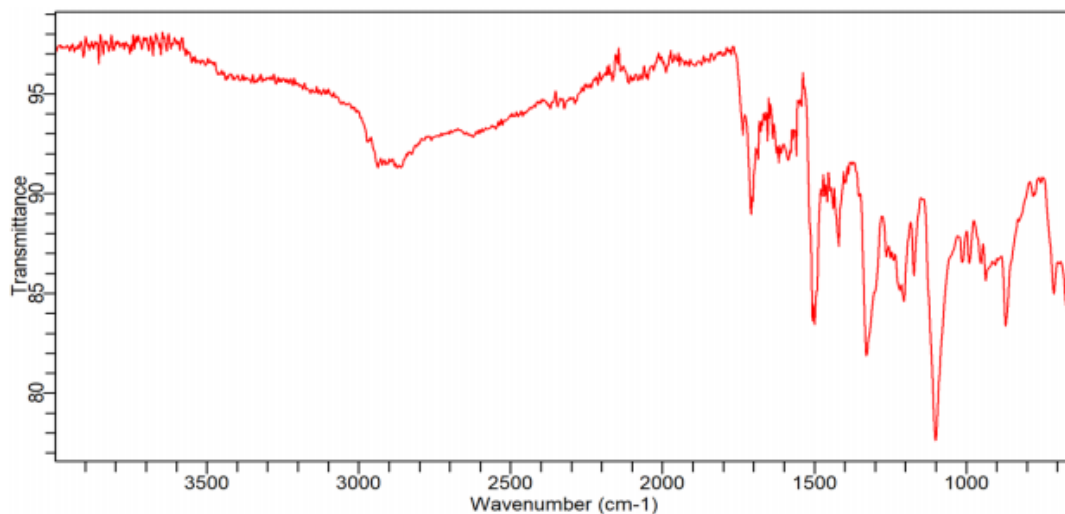
FT-IR spectra



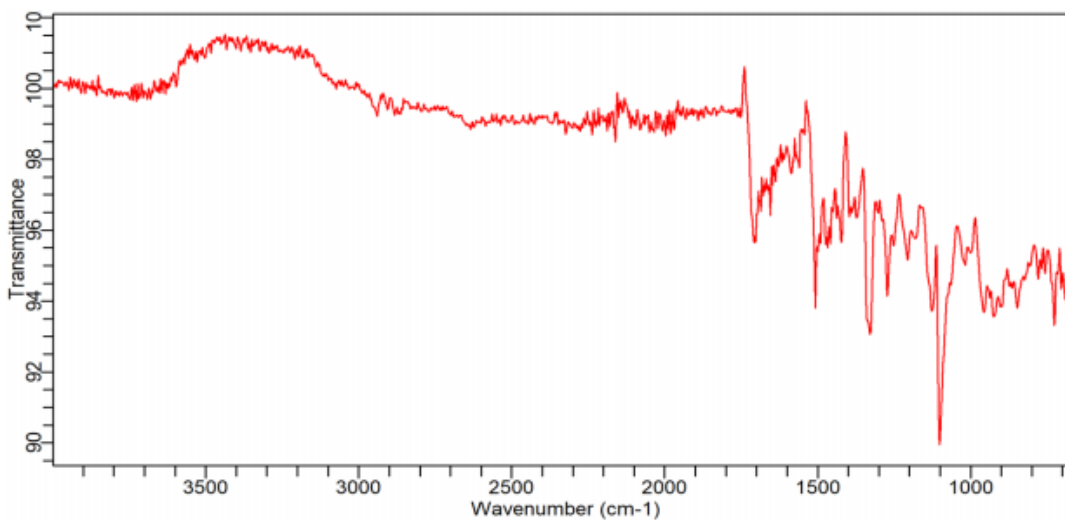
Annex 1. FT-IR spectrum of JH3, (2S)-2-[5-(6-{5-[(1S)-1-carboxy-3-methylbutyl]-2-thioxo-1,3,5-thiadiazin-3-yl}butyl)-6-thioxo-1,3,5-thiadiazin-3-yl]-4 methylpentanoic acid. On the X-axis are represented the wavenumber (cm⁻¹) vs. transmittance on the Y-axis.



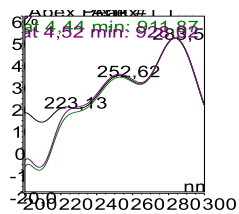
Annex 2. FT-IR spectrum of JH4, (2S)-2-[5-(6-{5-[(1S)-1-carboxy-3-methylbutyl]-2-thioxo-1,3,5-thiadiazin-3-yl}hexyl)-6-thioxo-1,3,5-thiadiazin-3-yl]-4 methylpentanoic acid. On the X-axis are represented the wavenumber (cm⁻¹) vs. transmittance on the Y-axis.



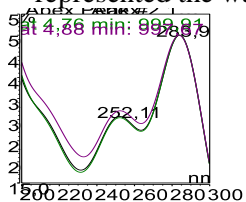
Annex 3. FT-IR spectrum of JH5, 2-(5-{6-[5-(1-carboxy-1-methylpropyl)-2-thioxo-1,3,5-thiadiazinan-3-yl]butyl}-6-thioxo-1,3,5-thiadiazin-3-yl)-3-methylbutanoic acid. On the X-axis are represented the wavenumber (cm^{-1}) vs. transmittance on the Y-axis.



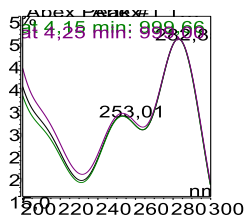
Annex 4. FT-IR spectrum of JH6, 2-(5-{6-[5-(1-carboxy-1-methylpropyl)-2-thioxo-1,3,5-thiadiazinan-3-yl] hexyl}-6-thioxo-1,3,5-thiadiazin-3-yl)-3-methylbutanoic acid. On the X-axis are represented the wavenumber (cm^{-1}) vs. transmittance on the Y-axis.



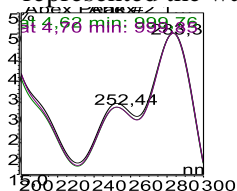
Annex 5. UV/Vis spectrum of JH3, (2S)-2-[5-(6-{5-[(1S)-1-carboxy-3-methylbutyl]-2-thioxo-1,3,5-thiadiazin-3-yl}butyl)-6-thioxo-1,3,5-thiadiazinan-3-yl]-4 methylpentanoic acid. On the X-axis are represented the wavelength (nm) vs. absorbance on the Y-axis.



Annex 6. UV/Vis absorption spectra of JH4, (2S) -2- [5- (6- {5 - [(1S) -1-carboxy-3-methylbutyl] - 2-thioxo-1,3,5-thiadiazinan-3-yl}hexyl)-6-thioxo-1,3,5-thiadiazinan-3-yl]-4 methylpentanoic acid. On the X-axis are represented the wavelength (nm) vs. absorbance on the Y-axis.

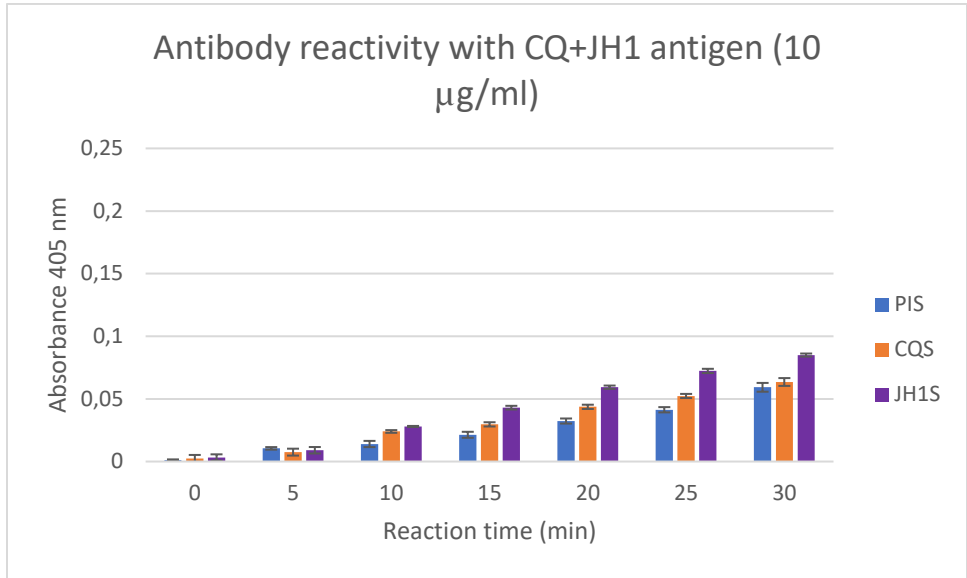


Annex 7. UV/Vis absorption spectra of JH5, 2-(5-{6-[5-(1-carboxy-1-methylpropyl)-2-thioxo-1,3,5-thiadiazinan-3-yl]butyl}-6-thioxo-1,3,5-thiadiazin-3-yl)-3-methylbutanoic acid. On the X-axis are represented the wavelength (nm) vs. absorbance on the Y-axis.

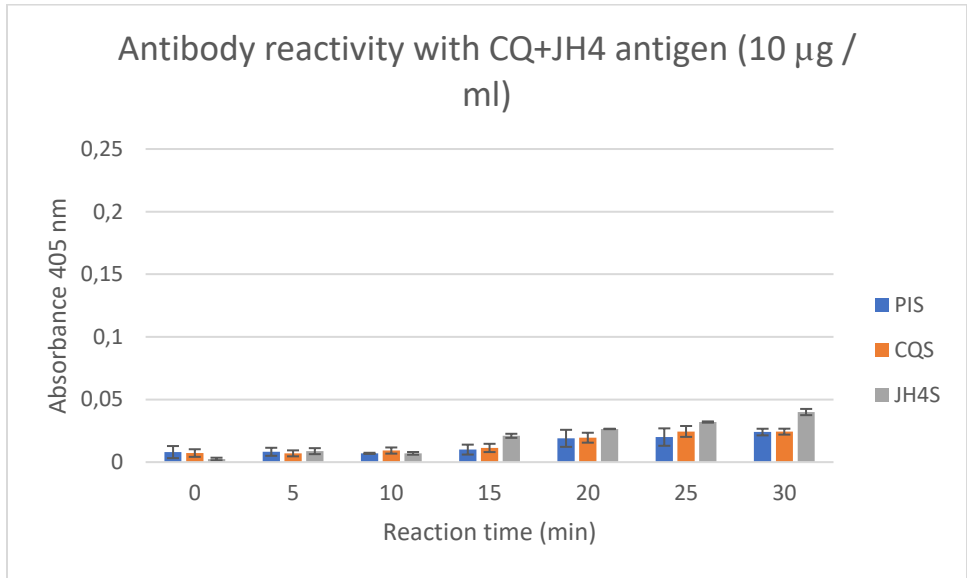


Annex 8. UV/Vis absorption spectra of JH6, 2-(5-{6-[5-(1-carboxy-1-methylpropyl)-2-thioxo-1,3,5-thiadiazinan-3-yl] hexyl}-6-thioxo-1,3,5-thiadiazin-3-yl)-3-methylbutanoic acid. On the X-axis are represented the wavelength (nm) vs. absorbance on the Y-axis.

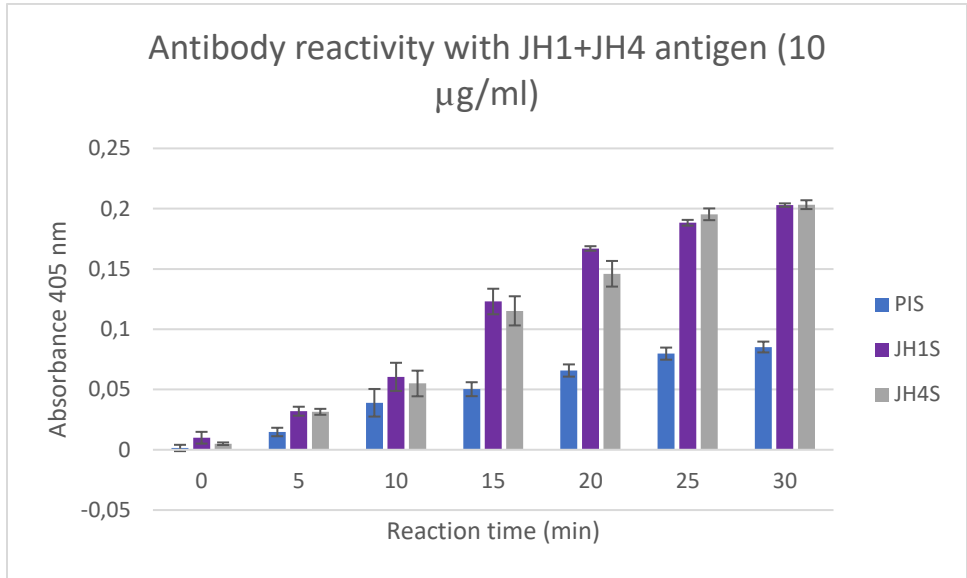
Evaluation for the reaction time of combination of antigens



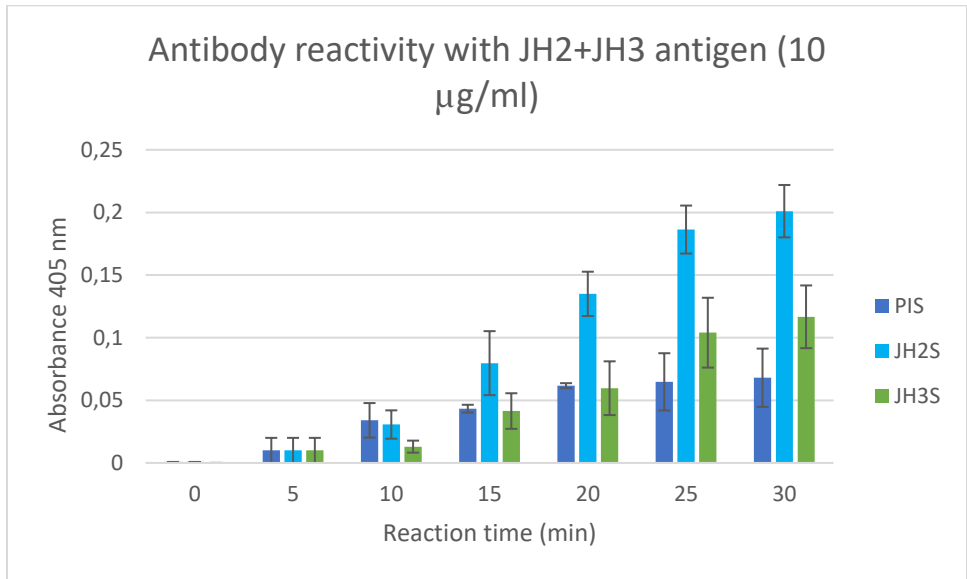
Annex 9. Indirect ELISA results, antibody (pre-immune called PIS and hyper-immune CQS, JH1S) reactivity with antigen (CQ+JH1 compounds). On the X-axis are represented the time of reading of reaction vs. absorbance at 405 nm on the Y-axis, and on the bars, the standard error is represented by a black line.



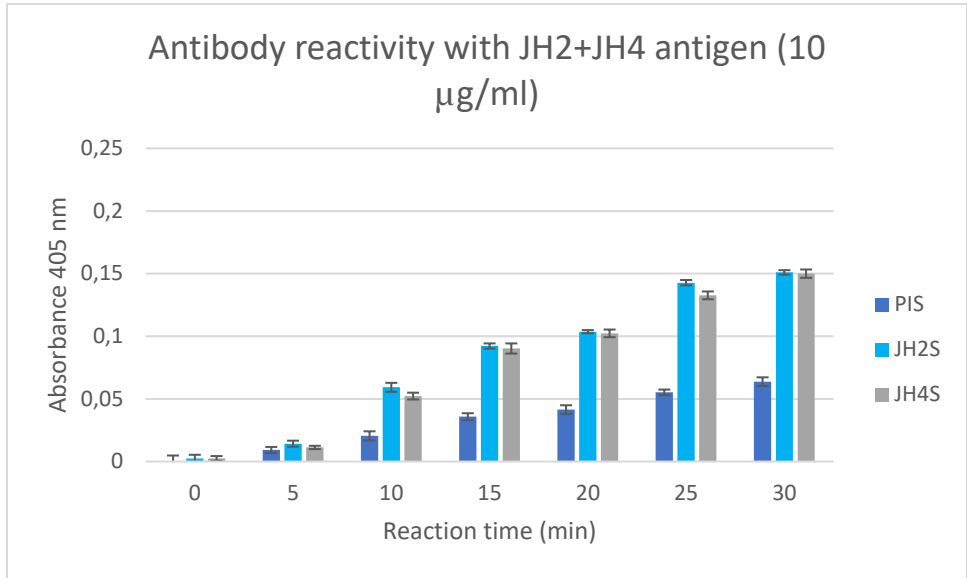
Annex 10. Indirect ELISA results, antibody (pre-immune called PIS and hyper-immune CQS, JH4S) reactivity with antigen (CQ+JH4 compounds). On the X-axis are represented the time of reading of reaction vs. absorbance at 405 nm on the Y-axis, and on the bars, the standard error is represented by a black line.



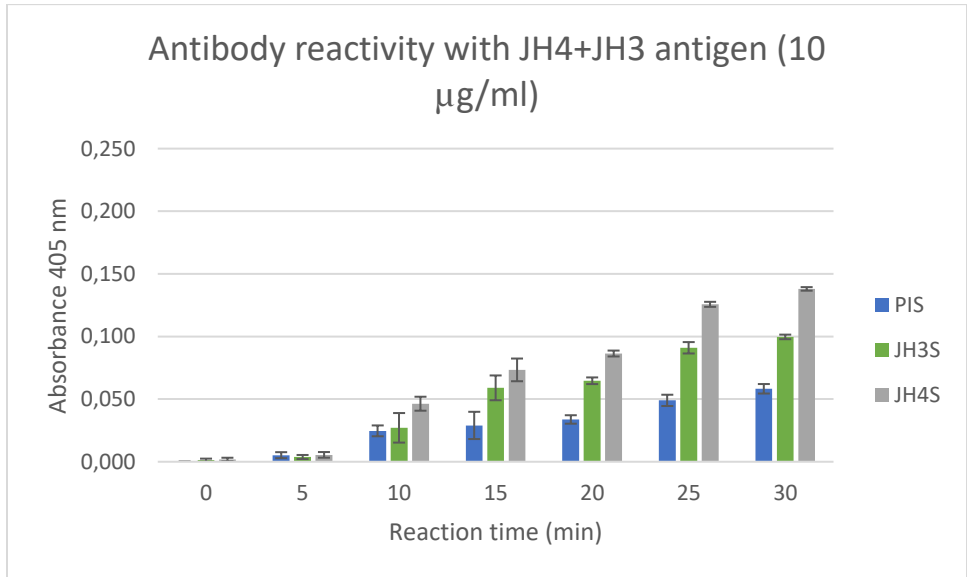
Annex 11. Indirect ELISA results, antibody (pre-immune called PIS and hyper-immune JH1S, JH4S) reactivity with antigen (JH1+JH4 compounds). On the X-axis are represented the time of reading of reaction vs. absorbance at 405 nm on the Y-axis, and on the bars, the standard error is represented by a black line.



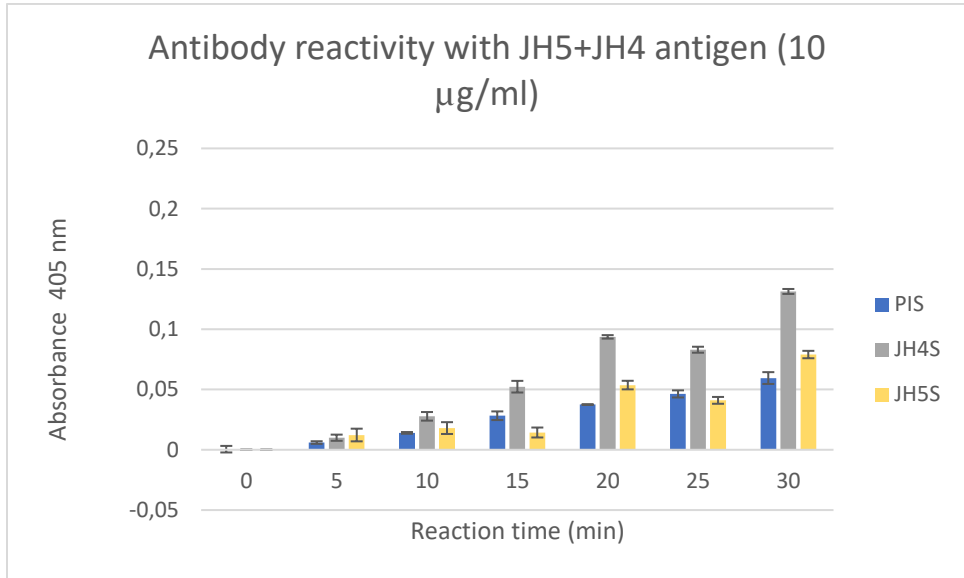
Annex 12. Indirect ELISA results, antibody (pre-immune called PIS and hyper-immune JH2S, JH3S) reactivity with antigen (JH2+JH3 compounds). On the X-axis are represented the time of reading of reaction vs. absorbance at 405 nm on the Y-axis, and on the bars, the standard error is represented by a black line.



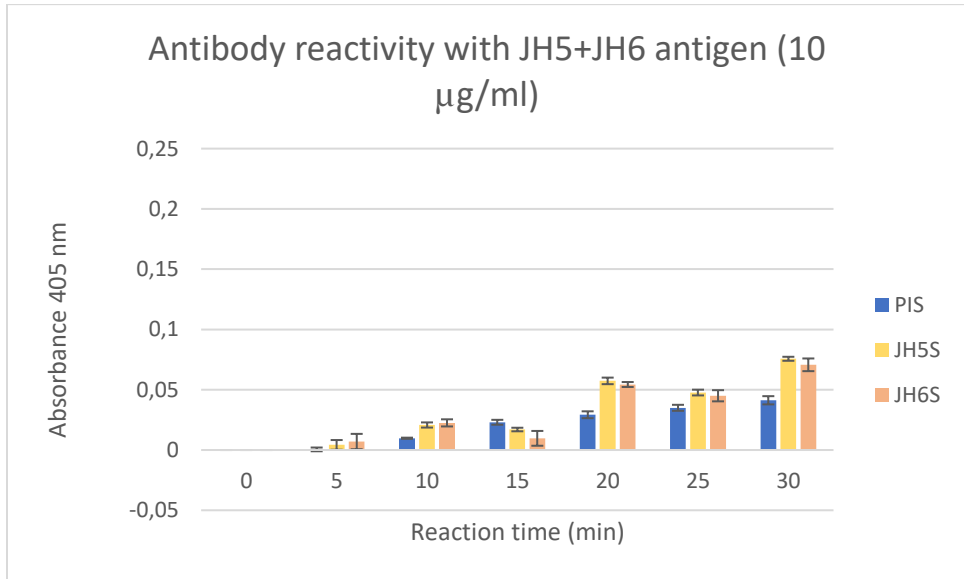
Annex 13. Indirect ELISA results, antibody (pre-immune called PIS and hyper-immune JH2S, JH4S) reactivity with antigen (JH2+JH4 compounds). On the X-axis are represented the time of reading of reaction vs. absorbance at 405 nm on the Y-axis, and on the bars, the standard error is represented by a black line.



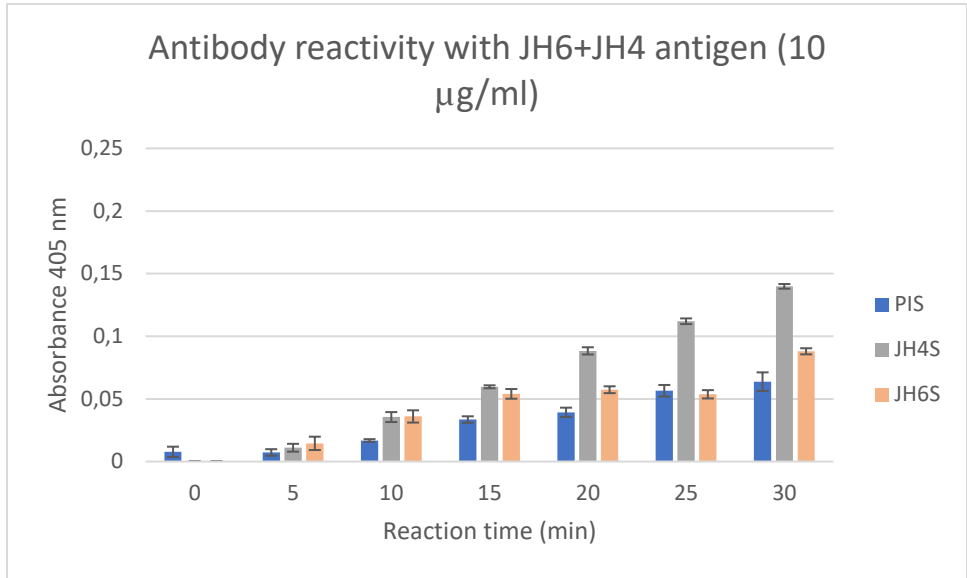
Annex 14. Indirect ELISA results, antibody (pre-immune called PIS and hyper-immune JH4S, JH3S) reactivity with antigen (JH4+JH3 compounds). On the X-axis are represented the time of reading of reaction vs. absorbance at 405 nm on the Y-axis, and on the bars, the standard error is represented by a black line.



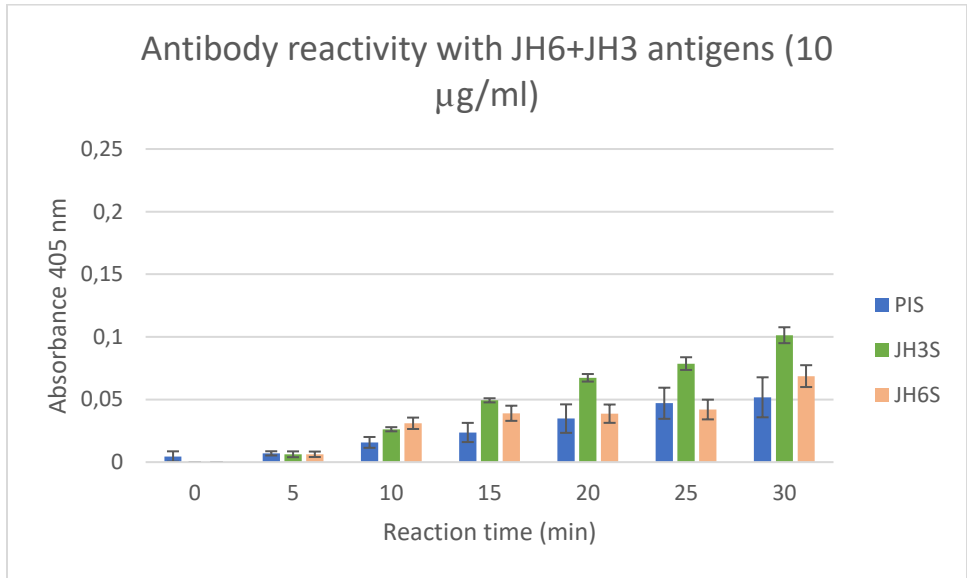
Annex 15. Indirect ELISA results, antibody (pre-immune called PIS and hyper-immune JH5S, JH4S) reactivity with antigen (JH5+JH4 compounds). On the X-axis are represented the time of reading of reaction vs. absorbance at 405 nm on the Y-axis, and on the bars, the standard error is represented by a black line.



Annex 16. Indirect ELISA results, antibody (pre-immune called PIS and hyper-immune JH5S, JH6S) reactivity with antigen (JH5+JH6 compounds). On the X-axis are represented the time of reading of reaction vs. absorbance at 405 nm on the Y-axis, and on the bars, the standard error is represented by a black line.



Annex 17. Indirect ELISA results, antibody (pre-immune called PIS and hyper-immune JH6S, JH4S) reactivity with antigen (JH6+JH4 compounds). On the X-axis are represented the time of reading of reaction vs. absorbance at 405 nm on the Y-axis, and on the bars, the standard error is represented by a black line.



Annex 18. Indirect ELISA results, antibody (pre-immune called PIS and hyper-immune JH6S, JH3S) reactivity with antigen (JH6+JH3 compounds). On the X-axis are represented the time of reading of reaction vs. absorbance at 405 nm on the Y-axis, and on the bars, the standard error is represented by a black line.